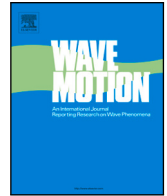


## Transformation-based cloaking for flexural-gravity waves in an anisotropic plate floating on shallow water

Sophie Thery, Malte A. Peter, Luke G. Bennetts, Sébastien Guenneau

### Angaben zur Veröffentlichung / Publication details:

Thery, Sophie, Malte A. Peter, Luke G. Bennetts, and Sébastien Guenneau. 2026. "Transformation-based cloaking for flexural-gravity waves in an anisotropic plate floating on shallow water." *Wave Motion* 140: 103642. <https://doi.org/10.1016/j.wavemoti.2025.103642>.



# Transformation-based cloaking for flexural–gravity waves in an anisotropic plate floating on shallow water<sup>☆</sup>

Sophie Thery <sup>a</sup>, Malte A. Peter <sup>a,b</sup>, Luke G. Bennetts <sup>c</sup>, Sébastien Guenneau <sup>d</sup>

<sup>a</sup> Institute of Mathematics, University of Augsburg, Universitätsstraße 12a, Augsburg, 86159, Germany

<sup>b</sup> Centre for Advanced Analytics and Predictive Sciences, University of Augsburg, Universitätsstraße 12a, Augsburg, 86159, Germany

<sup>c</sup> School of Mathematics and Statistics, University of Melbourne, Melbourne, VIC 3010, Australia

<sup>d</sup> Blackett Laboratory, Physics Department, UMI 2004 Abraham de Moivre-CNRS, Imperial College London, South-Kensington, London, SW7 2AZ, UK

## ARTICLE INFO

MSC:  
35J55  
74F10

### Keywords:

Anisotropic Kirchhoff–Love plate  
Cloaking  
Flexural–gravity waves  
Shallow water

## ABSTRACT

The principle of cloaking has been developed and applied to different types of waves. We consider the application in the context of flexural–gravity waves on shallow water in order to reduce the wave force on an object. The parameters of the plate used to create a cloak in the vicinity of the object are found applying a space transformation method to the wave-propagation equation. The governing equation of a Kirchhoff–Love plate is generally not shape-invariant, which traditionally induces error terms in the (thus approximate) use of the space transformation method. First deriving the equations of motion for the shallow-water-fully anisotropic plate system by a variational principle, we extend the transformation method to anisotropic plates and show that for every change of coordinates there exists a class of anisotropic plates such that the equation of motion is shape-invariant. Furthermore, we consider examples in which the wave force on and the scattering by a rigid bottom-mounted vertical cylinder are reduced when surrounded by a floating plate with a cloaking region having material parameters computed by the presented method and we illustrate an approximate case by simulations.

## 1. Introduction

The cloaking principle was developed with the aim of bending electromagnetic waves around an object, such that the object is invisible to an observer located away from the object [1,2]. The material that surrounds the object and allows this deviation of the path of the waves is called the *cloak*, and the so-called *space transformation method* for determining the properties of the cloaking material is based on a change of coordinates in the equations governing wave propagation [3]. The usual approach is to *transform* coordinates from an isotropic material to an *arrival space* obtained by inflating a point of very small diameter (and, thus, negligible scattering). This creates annular cloaking regions consisting of anisotropic materials, which are typically realised using metamaterials acting in an effective sense by designing their microstructure appropriately [4,5]. The space transformation method relies on the equation governing wave propagation being shape-invariant, which means the structure of the mathematical operators in the governing equation remains unchanged by the transformation. The principle has been applied to numerous types of waves, such as acoustic waves [6,7], and shallow-water waves [8,9].

<sup>☆</sup> This article is part of a Special issue entitled: ‘KOZWaves24’ published in Wave Motion.

\* Corresponding author.

E-mail address: [sophie.thery@insa-lyon.fr](mailto:sophie.thery@insa-lyon.fr) (S. Thery).

<https://doi.org/10.1016/j.wavemoti.2025.103642>

Received 30 December 2024; Received in revised form 1 July 2025; Accepted 12 September 2025

Available online 20 September 2025

0165-2125/© 2025 The Authors. Published by Elsevier B.V. This is an open access article under the CC BY license (<http://creativecommons.org/licenses/by/4.0/>).

In the context of water waves, the primary motivation for creating a cloak is for the ocean engineering application of reducing wave forces on an offshore structure [9]. However, the difficulty in applying the space transformation method to water waves is that the general (linear) water-wave system is not shape-invariant, so the space transformation method cannot be directly applied [8,10]. Nevertheless, in the shallow-water regime that is relevant to near-shore ocean engineering, the governing equations are shape-invariant at the price of non-homogeneous and possibly anisotropic coefficients in the transformed equations, such as the transformed water height.

The space transformation method was applied in its general form in the shallow-water regime by [11] and they proposed a specific transformation that requires only anisotropic bathymetry to design the cloak. Subsequent design and numerical simulations were performed by [12,13]. Based on the transformation method, anisotropy is realised by structures in the water or by a change of the bathymetry, e.g. [14] suggest an assembly of rigid cylinders clamped to a flat seabed and piercing the free-water surface, whereas [15] realise the cloak by a change in seabed topography. In the context of the mild-slope approximation [16], design and numerical simulation of a structure cloaking a bottom-mounted cylinder by bathymetry variations and surface-piercing structures using a homogenisation technique were presented by [17]. In [18], a design of a channel network to attain water-wave cloaking was proposed. Moreover, an experimental realisation of a waveguide in the shallow-water regime using anisotropic bathymetry was described by [19].

For the case of a vertical cylinder in water, a cloaking approach based on direct numerical optimisation (rather than space transformation) was suggested by [10,20]. They optimised the bathymetry in the context of a mild-slope approximation by cancelling the scattering. Similarly, [21] optimised surface-piercing structures surrounding a vertical cylinder and a flat seabed. Nonetheless, the direct approach has the disadvantage of being dependent on the cloaked object and the frequency of the incoming waves.

It would be challenging and costly to build and deploy bottom-mounted structures or to adjust the bathymetry to create a cloak. Therefore, attention has turned to use of floating elastic plates to achieve cloaking. Using the direct numerical optimisation approach, [22] cloaked a cylinder in water of finite depth by finding the optimal multilayer isotropic plate that reduces scattering. However, the space transformation method seems not to have been applied to design a cloak made up of a floating plate yet. Indeed, it is well-known that the space transformation method cannot, in general, be applied to elastic plates (even without fluid loading), as the equation for the wave motion is not shape-invariant [23–25]. More precisely, [23] show that the equations governing wave propagation in elastic materials are only shape-invariant for general elastic materials with an additional pre-stress term. It is unknown how to handle the space transformation method for a thin plate with no additional pre-stress, although approximate cloaking has been experimentally achieved in structured plates [26–28]. Analytically, different strategies were proposed to approximate a perfect cloak within a plate, such that the cloak is the result of a shape-invariant transformation. For example, [29] developed a model for general orthotropic elastic materials, i.e. anisotropy is along orthogonal axes, and compared membrane equations with plate equations. Also, [30] considered orthotropic plates and determined a particular change of coordinates to create an approximate but efficient cloak. Both attempts resulted in imperfect cloaks because some terms corresponding to the pre-stress force are neglected in the final cloak. Nevertheless, they showed that the error made by the approximation decreases with the penetration depth of the wave into the cloak, resulting in efficient cloaking. Finally, [31] proposed an alternative approach by using the variational formulation of the equations of motion, making it easier to handle the terms that make the equation non-shape-invariant since the rigidity tensor can be rewritten as a bilinear form in the variational formulation. The authors pointed out that the biharmonic equation should be shape-invariant for a class of transformations with a vanishing Hessian.

Here, starting from an anisotropic plate, we devise a transformation method which does not require to search for a specific transformation minimising the pre-stress terms or even having vanishing Hessians. Using this novel approach, we resolve the issue of the non-shape-invariant form of the Kirchhoff–Love plate equation by generalising the concept to the fully anisotropic plate (i.e. with anisotropic rigidity and thickness), paying special attention to boundary terms before coupling to the shallow-water system. We then apply the transformation method for general transformations and anisotropic plates and we show that, for every change of coordinates, one can find a class of anisotropic plates that make the equation shape-invariant. We derive the model of the fully anisotropic floating plate using Hamilton’s principle for the Kirchhoff–Love plate. In particular, the general boundary condition for the fully anisotropic plate with arbitrary boundary is derived. Application of the cloaking principle is given in the context of an infinite floating plate in the shallow-water regime. It turns out that, because of the coupling of two physical domains (plate and water), both the rigidity of the plate and water height have to be anisotropic in the cloak. To allow for a constant seabed, the cloak is created using a plate with anisotropic rigidity and immersion. Our cloaking strategy is illustrated based on the obtained parameters without discussing how to create a plate with these parameters. Finally, we give an approximate numerical example showing that the cloak leads to reduction of wave forcing on and scattering of a bottom-mounted cylinder subjected to incident flexural-gravity waves.

The plan of the paper is as follows. We first construct the model of a floating anisotropic plate using a variational approach in Section 2. We build our model first for an in-vacuo plate (Section 2.1) and for water waves in shallow water (Section 2.2) separately, before coupling them to a model for a floating plate (Section 2.3). The change of coordinates is applied to the variational formulation of the final model in Section 3. This transformation leads to a new floating plate with anisotropic rigidity and anisotropic immersion (Section 3.1). We detail the computation for the elastic part that is not shape-invariant in general (Section 3.2). However, we show in Section 3.3 that for all changes of coordinates we can find anisotropic plate parameters such that the elastic part is shape-invariant. Formulas to find such plate parameters are given in that section. We explain in Section 4 how the method is applied to the plate floating on shallow water. The approximate numerical example to illustrate our results is given in Section 5. We end with some conclusions and an outlook in Section 6.

## 2. Floating elastic plate model

In order to manipulate the formulations for a change of coordinates for the anisotropic plate and build our method more easily, we work with a variational formulation derived from an associated Lagrangian and use Hamilton's principle. This approach was used in [32,33] for an isotropic plate in the context of modelling water-wave interactions with sea ice. Here, we extend the variational formulation to a general anisotropic Kirchhoff–Love plate, which may also serve as a useful reference outside the cloaking context. The construction is split into first giving the variational form for the anisotropic plate in Section 2.1, then for the water domain in Section 2.2, where the shallow-water approximation is assumed, and finally for the coupled model of a plate floating on shallow water in Section 2.3.

### 2.1. Variational formulation of the anisotropic thin plate

We suppose a horizontal thin plate occupying  $\Omega \times (-p, P - p)$  in three spatial dimensions with Cartesian coordinates  $(x_1, x_2, x_3)$ , where  $\Omega \subseteq \mathbb{R}^2$  and  $p = p(x_1, x_2)$  and  $P = P(x_1, x_2)$  are functions denoting the local distance of the bottom of the plate from the  $\{x_3 = 0\}$ -plane and the thickness of the plate at rest, respectively (see Fig. 1 for an illustration). This description of the geometry will prove useful when adding the water domain, in which case  $p$  reflects the local submergence.

We assume the thin-plate approximation within the Kirchhoff–Love plate theory to be valid, so that the momentum is defined as  $M_{ij} = \int_{-p}^{P-p} x_3 \sigma_{ij}$ , where  $\sigma_{ij}$  are the stresses,  $i, j = 1, 2$ . The (local) flexural rigidity tensor of the plate is denoted by  $D_{ijkl}$  and  $M_{ij} = D_{ijkl} w_{,kl}$  with  $w$  the vertical (out-of-plane) displacement depending on horizontal variables  $x_i$ ,  $i \in \{1, 2\}$ . Here and in what follows, we use Einstein notation so that  $\cdot_{,i}$  denotes the derivative in the  $i$ th spatial coordinate and  $\cdot_{,i}$  denotes the derivative with respect to time  $t$ . Similarly,  $\cdot_{,ij}$  denotes the second-order derivative in the  $i$ th and  $j$ th spatial coordinates and  $\cdot_{,ii}$  denotes the second-order derivative with respect to time. With standard symmetries  $D_{ijkl} = D_{klij} = D_{jikl} = D_{ijlk}$ , see e.g. [34], we have  $M_{12} = M_{21}$  and

$$\begin{pmatrix} M_{11} \\ M_{22} \\ M_{12} \end{pmatrix} = \begin{pmatrix} D_{1111} & D_{1122} & 2D_{1112} \\ D_{1122} & D_{2222} & 2D_{2221} \\ D_{1112} & D_{2221} & 2D_{1212} \end{pmatrix} \begin{pmatrix} w_{,11} \\ w_{,22} \\ w_{,12} \end{pmatrix}. \tag{1}$$

The Lagrangian of the plate is given by the difference of the elastic energy and the kinetic energy,

$$\mathbf{L}_p(w) = \int_{\Omega} -\frac{1}{2} w_{,ij} D_{ijkl} w_{,kl} + \frac{1}{2} \rho_0 P(w_{,t})^2 dx_1 dx_2,$$

where  $\rho_0$  is the density of the plate. The variation of the Lagrangian is given by

$$\delta \mathbf{L}_p(w, \delta w) = \int_{\Omega} -\delta w_{,ij} D_{ijkl} w_{,kl} + \rho_0 P w_{,t} \delta w_{,t} dx_1 dx_2. \tag{2}$$

Integrating with respect to time and integrating by parts with respect to time, we obtain the variation of the action,  $\delta \mathbf{S}_p$ , as

$$\delta \mathbf{S}_p(w, \delta w) = - \int_{t_0}^{t_1} \left( \int_{\Omega} \delta w_{,ij} D_{ijkl} w_{,kl} + \rho_0 P w_{,tt} \delta w \right) dx_1 dx_2 dt. \tag{3}$$

To derive the free boundary conditions, we integrate by parts with respect to space twice as detailed in Appendix A to obtain

$$\delta \mathbf{S}_p(w, \delta w) = - \int_{t_0}^{t_1} \left( \int_{\Omega} \delta w \left( (M_{ij})_{,ij} + \rho_0 P w_{,tt} \right) dx_1 dx_2 - BC(w, \delta w) \right) dt, \tag{4a}$$

$$BC(w, \delta w) = \int_{\partial \Omega} \left( \mathbf{n}^T \begin{pmatrix} M_{11} & \frac{1}{2} M_{12} \\ \frac{1}{2} M_{12} & M_{22} \end{pmatrix} \mathbf{n} \right) (\nabla_h \delta w \cdot \mathbf{n}) + \left( \mathbf{s}^T \begin{pmatrix} M_{11} & M_{12} \\ M_{12} & M_{22} \end{pmatrix} \mathbf{n} \right) (\nabla_h \delta w \cdot \mathbf{s}) - \delta w \begin{pmatrix} M_{11,1} + M_{12,2} \\ M_{12,1} + M_{22,2} \end{pmatrix} \cdot \mathbf{n}, \tag{4b}$$

with  $\nabla_h$  denoting the gradient with respect to horizontal coordinates  $x_1, x_2$ ,  $M$  the momentum defined in (1),  $\mathbf{n}$  the normal vector to  $\partial \Omega$  and  $\mathbf{s}$  the tangential direction. These boundary conditions are consistent with the boundary conditions given by [35,36]. After integration by parts in the term involving  $\nabla_h \delta w \cdot \mathbf{s}$ ,  $BC$  is rewritten as

$$BC(w, \delta w) = \int_{\partial \Omega} \left( \mathbf{n}^T \begin{pmatrix} M_{11} & M_{12} \\ M_{12} & M_{22} \end{pmatrix} \mathbf{n} \right) (\nabla_h \delta w \cdot \mathbf{n}) - \delta w \left[ \begin{pmatrix} M_{11,1} + M_{12,2} \\ M_{12,1} + M_{22,2} \end{pmatrix} \cdot \mathbf{n} + \nabla_h \left( \mathbf{s}^T \begin{pmatrix} M_{11} & M_{12} \\ M_{12} & M_{22} \end{pmatrix} \mathbf{n} \right) \cdot \mathbf{s} \right]. \tag{5}$$

We note that, for the special case of an isotropic homogeneous plate ( $D_{1111} = D_{2222} = D$ ,  $D_{1112} = D_{2221} = 0$ ,  $D_{1122} = \nu D$  and  $D_{1212} = (1 - \nu)D/2$ , with  $\nu, D$  constant), boundary conditions (5) represent the standard free-edge boundary conditions [37]. The complete computation in the isotropic case can be found in [32].

### 2.2. Variational formulation for the water

Consider a free surface (no plate) water domain  $\Omega_w := \{(x_1, x_2, x_3) \in \mathbb{H} \times \mathbb{R} \mid -d \leq x_3 \leq \eta(t, x_1, x_2)\}$ , where  $\mathbb{H} \subseteq \mathbb{R}^2$  and for a constant seabed depth  $d$  and local surface displacement  $\eta$ . Full construction of the functional for surface waves for water of finite

depth can be found in [38] or [39]. The Lagrangian for the free surface water in  $\Omega_w$  is  $L_w = \int_{\Omega_w} p_w$ , where  $p_w$  is the water pressure. Using Bernoulli's equation, the Lagrangian becomes

$$\begin{aligned} L_w(\Phi, \eta) &= -\rho_w \int_{\mathbb{H}} \int_{-d}^{\eta} \Phi_{,t} + gz + \frac{1}{2} |\nabla\Phi|^2 \, dx_3 dx_1 dx_2 \\ &= \rho_w \int_{\mathbb{H}} \left[ -\partial_t \left( \int_{-d}^{\eta} \Phi dx_3 \right) + \eta_{,t} \Phi_{\eta} - \frac{1}{2} g (\eta^2 - d^2) - \frac{1}{2} \left( \int_{-d}^{\eta} |\nabla\Phi|^2 \, dx_3 \right) \right] dx_1 dx_2, \end{aligned} \tag{6}$$

where  $\rho_w$  is the water density,  $g$  is the constant of gravitational acceleration,  $\Phi_{,\eta}$  is short-hand for  $\Phi(x_1, x_2, \eta(x_1, x_2))$  and  $\Phi$  is the water velocity potential, the gradient of which gives the water velocity (having assumed irrotational motion).

Integrating over a time interval  $[t_0, t_1]$  and fixing the (arbitrary) normalisation of the potential such that  $\left[ \int_{\Omega_w} \Phi \right]_{t_0}^{t_1} = 0$ , we obtain the action

$$S_w(\Phi, \eta) = \rho_w \int_{t_0}^{t_1} \left( \int_{\mathbb{H}} \eta_{,t} \Phi_{\eta} - \frac{1}{2} g (\eta^2 - d^2) - \frac{1}{2} \int_{-d}^{\eta} |\nabla\Phi|^2 \, dx_3 dx_1 dx_2 \right) dt. \tag{7}$$

The first variation of the functional is

$$\delta S_w(\delta\Phi, \Phi, \eta, \delta\eta) = \rho_w \int_{t_0}^{t_1} \left( \int_{\mathbb{H}} \delta\Phi_{,\eta} \eta_{,t} + \Phi_{,\eta} \delta\eta_{,t} - g\eta\delta\eta - \int_{-d}^{\eta} \nabla\delta\Phi \cdot \nabla\Phi dx_3 + \frac{1}{2} \delta\eta |\nabla\Phi|^2 \, dx_1 dx_2 \right) dt. \tag{8}$$

Using Green's formula in the term containing  $\nabla\delta\Phi \cdot \nabla\Phi$ , we can derive the boundary and surface conditions,

$$\begin{aligned} - \int_{\mathbb{H}} \int_{-d}^{\eta} \nabla\delta\Phi \cdot \nabla\Phi \, dx_1 dx_2 dx_3 &= \int_{\mathbb{H}} \int_{-d}^{\eta} \delta\Phi \Delta\Phi \, dx_1 dx_2 dx_3 + \int_{\mathbb{H}} \delta\Phi_{-d} \Phi_{-d,3} + \delta\Phi_{,\eta} (-\nabla_{\eta} \eta \cdot \nabla_{\mathbb{H}} \Phi_{,\eta} + \Phi_{,\eta,3}) \, dx_1 dx_2 \\ &\quad + \int_{\partial\mathbb{H}} \delta\Phi \nabla_{\mathbb{H}} \Phi \cdot \mathbf{n} \, dx_3, \end{aligned} \tag{9}$$

where, as before,  $\nabla_{\mathbb{H}}$  is the gradient operator with respect to the horizontal coordinates. Integrating by parts the term with  $\delta\eta_{,t}$  in (8), injecting (9) and linearising for small elevation  $\eta$  around  $z = -p$  (note that  $p = 0$  in the classic free surface case) gives the first variation for the water domain,

$$\begin{aligned} \delta S_w(\delta\Phi, \Phi, \eta, \delta\eta) &= \rho_w \int_{t_0}^{t_1} \left( \int_{\mathbb{H}} \int_{-d}^{-p} \delta\Phi \Delta\Phi \, dx_3 - \delta\Phi_{-p} (\nabla_{\mathbb{H}} p \cdot \nabla_{\mathbb{H}} \Phi_{-p} + \Phi_{-p,3} - \eta_{,t}) \right. \\ &\quad \left. - \delta\eta (\Phi_{-p,t} + g\eta) + \delta\Phi_{-d} \Phi_{-d,3} \, dx_1 dx_2 + \int_{\partial\mathbb{H}} \delta\Phi \nabla_{\mathbb{H}} \Phi \cdot \mathbf{n} \right) dt. \end{aligned} \tag{10}$$

It is well-known that the formulation (10) is not shape-invariant and we refer to [8,10] for discussion and details on this point. To be able to use the space transformation method in what follows, we pass to a shallow-water regime, which is shape-invariant at the expense of having to adjust the local water height  $H := d - p$ , [11]. Therefore, we restrict to wavelengths much greater than the water height, and, to derive the variational form in the shallow regime, we adopt the formulation derived by [40], such that

$$\nabla\Phi = \mathbf{u} = \left( \begin{array}{c} \mathbf{u}_{\mathbb{H}}(x_1, x_2, t) \\ \left( \frac{x_3 + p + 1}{H} \right) (\eta_{,t} + \nabla_{\mathbb{H}} H \cdot \mathbf{u}_{\mathbb{H}}) \end{array} \right), \tag{11}$$

in which  $\mathbf{u}_{\mathbb{H}}$  denotes the vector of horizontal velocities. Injecting (11) in (10) makes the terms involving  $\delta\Phi_{-d}$  and  $\delta\Phi_{-p}$  disappear and the volume term in the functional for the water becomes

$$\int_{-d}^{-p} \delta\Phi \Delta\Phi dx_3 = \left( \int_{-d}^{-p} \frac{\delta\Phi}{H} dx_3 \right) (\eta_{,t} + \nabla_{\mathbb{H}} \cdot (H \mathbf{u}_{\mathbb{H}})). \tag{12}$$

Denoting  $\Psi(\delta\Phi) = \int_{-d}^{-p} \frac{\delta\Phi}{H} dx_3$ , the variational formulation for shallow water is given by

$$\delta S_{sw}(\Phi, \delta\Phi, \eta, \delta\eta) = \rho_w \int_{t_0}^{t_1} \left( \int_{\mathbb{H}} \Psi(\delta\Phi) (\eta_{,t} + \nabla_{\mathbb{H}} \cdot (H \nabla_{\mathbb{H}} \Phi)) - \delta\eta (\Phi_{,t} + g\eta) \, dx_1 dx_2 - \int_{\partial\mathbb{H}} \delta\Phi \nabla_{\mathbb{H}} \Phi \cdot \mathbf{n} \right) dt. \tag{13}$$

### 2.3. Floating plate on water variational model

Now, we combine the variational formulations for the plate and the water to obtain a variational model for a plate floating on shallow water. We assume the water surface is in contact with the plate immersion  $-p$  at all times, so that the water-surface elevation  $\eta$  is equal to the plate displacement  $w$  and  $\mathbb{H} = \Omega$ . The two variational formulations can be combined considering the water as an external force on the plate in terms of the pressure. Thus, the Lagrangian for the total system is  $L = L_p + L_w$  and the first variation of the functional for the full floating plate system is given by

$$\begin{aligned} \delta S(\delta\Phi, \Phi, \eta, \delta\eta) &= \delta S_w(\delta\Phi, \Phi, \eta, \delta\eta) + \delta S_p(\delta\Phi, \Phi, \eta, \delta\eta) \\ &= \int_{t_1}^{t_2} \int_{\Omega} \rho_w \Psi(\delta\Phi) (\eta_{,t} + \nabla_{\mathbb{H}} \cdot (H \nabla_{\mathbb{H}} \Phi)) - \delta\eta (\rho_w \Phi_{,t} + \rho_w g\eta + (D_{ijkl} \eta_{,kl})_{,ij} + \rho_0 P \eta_{,tt}) \, dx_1 dx_2 \end{aligned} \tag{14}$$

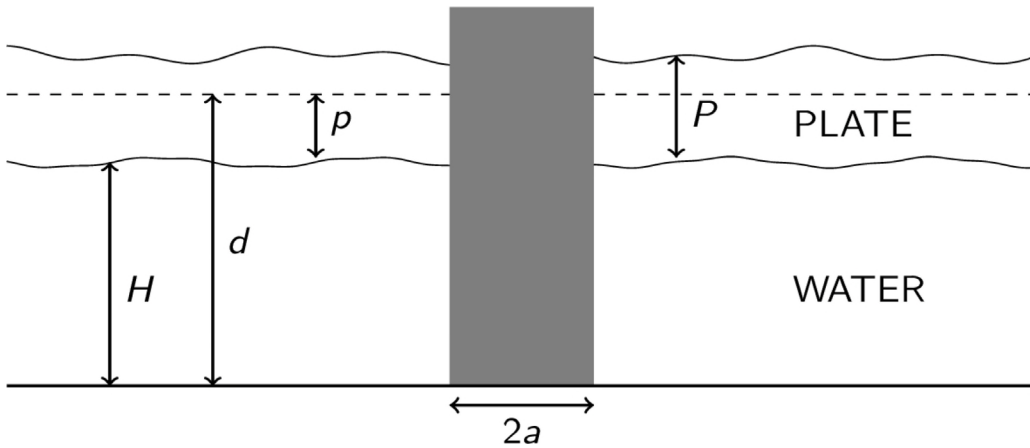


Fig. 1. Schematic diagram of the cross-section of a floating plate surrounding a bottom-mounted circular cylinder (grey region).

$$- \int_{\partial\Omega} \rho_w \delta\Phi \nabla_h \Phi \cdot \mathbf{n} - BC(\eta, \delta\eta) \Big] dt.$$

Another way to construct the coupled model is to consider the pressure exerted by the object on the fluid as a Lagrange multiplier associated with the constraint  $w = \eta$  as proposed by [41].

In what follows, we will also consider the problem where a rigid bottom-mounted vertical circular cylinder of radius  $a$  centred at the origin pierces the floating plate, so that  $\Omega = \{(x_1, x_2) \in \mathbb{R}^2, x_1^2 + x_2^2 > a^2\}$ . To simplify the time dependence and to focus on the spatial change of coordinates, we restrict the study to time-harmonic motions, so that  $\eta = \Re\{e^{-i\alpha t} \xi\}$  and  $\Phi = \Re\{e^{-i\alpha t} \phi\}$  with complex-valued spatial parts  $\xi$  and  $\phi$  of the original quantities and radian frequency  $\alpha$ . For the scattering problem, the incident wave is given by the potential  $\Phi_{\text{inc}} = \Re\{e^{-i\alpha t} \phi_{\text{inc}}\}$ .

We also note that it is possible to generalise the model to a fully anisotropic plate, which involves anisotropic thickness  $\mathbf{P}$ , anisotropic density  $\rho_0$  and, consequently, anisotropic water height  $\mathbf{H}$ . As mentioned before, these anisotropic parameters must be interpreted as effective parameters, for example resulting from the rational design and homogenisation of a multiscale structure [42,43]. Taking this general form and according to (14), the system of equations of motion becomes

$$-i\alpha\xi + \nabla \cdot (\mathbf{H}\nabla\phi) = 0 \quad \text{on } \Omega, \tag{15a}$$

$$-i\alpha\rho_w\phi + \rho_w g\xi + (M_{ij}(\xi))_{,ij} - \langle \rho_0, \mathbf{P} \rangle \alpha^2 \xi = 0 \quad \text{on } \Omega, \tag{15b}$$

$$\nabla\phi \cdot \mathbf{n} = 0 \quad \text{on } \partial\Omega, \tag{15c}$$

$$\mathbf{n}^T \begin{pmatrix} M_{11}(\xi) & M_{12}(\xi) \\ M_{12}(\xi) & M_{22}(\xi) \end{pmatrix} \mathbf{n} = 0 \quad \text{on } \partial\Omega, \tag{15d}$$

$$\begin{pmatrix} M_{11,1}(\xi) + M_{12,2}(\xi) \\ M_{12,1}(\xi) + M_{22,2}(\xi) \end{pmatrix} \cdot \mathbf{n} + \nabla \cdot \left( \mathbf{s}^T \begin{pmatrix} M_{11}(\xi) & M_{12}(\xi) \\ M_{12}(\xi) & M_{22}(\xi) \end{pmatrix} \mathbf{n} \right) \cdot \mathbf{s} = 0 \quad \text{on } \partial\Omega, \tag{15e}$$

$$\phi - \phi_{\text{inc}} \text{ satisfy radiation conditions} \tag{15f}$$

with  $\mathbf{n} = (\cos(\theta), \sin(\theta))^T$  and  $\mathbf{s} = (-\sin(\theta), \cos(\theta))^T$  and  $\langle \rho_0, \mathbf{P} \rangle = \rho_{0ij} P_{ij}$  denotes the Frobenius inner product. Here and in what follows, we have dropped the subscripts  $h$  of the gradients for notational convenience. We note that, to solve the system, it is convenient to inject (15a) into (15b) and obtain an equation for the potential  $\phi$  only,

$$\alpha^2 \rho_w \phi + \rho_w g \nabla \cdot (\mathbf{H}\nabla\phi) - \langle \rho_0, \mathbf{P} \rangle \alpha^2 \nabla \cdot (\mathbf{H}\nabla\phi) + (M_{ij}(\nabla \cdot (\mathbf{H}\nabla\phi)))_{,ij} = 0 \tag{16}$$

with boundary conditions (15c)–(15e) rewritten for  $\phi$  accordingly.

*Remark.* To the best of our knowledge, a proof of mathematical well-posedness for this problem of a fully anisotropic floating plate does not exist in the literature. We refer to [44] for the well-posedness of the isotropic Kirchhoff–Love plate equation alone with radiation condition and [45] for the infinite plate case. We will not treat the problem of well-posedness for the general case in this paper. Nonetheless, we give an example in Section 5 for a specific anisotropic plate where a solution is computed using the eigenfunction matching method.

### 3. Change of coordinates and shape-invariant form

The idea of transformation-based cloaking is to start with the desired problem setup but only containing a small (or even vanishing) version of the scatterer, which produces negligible scattering owing to its small size (or none at all). The spatial domain

containing the scatterer and its surroundings are then transformed in a way such that the scatterer is enlarged to its real size. Clearly, as part of this transformation, the equations of motions in the domain surrounding the scatterer transform. If the equations are shape-invariant, the transformation is only reflected in changed (local) material parameters but not in the structure of the equations. In a medium with these transformed material parameters, the scattering by the real-sized scatterer is still negligible.

In order to apply transformation-based cloaking, we suppose a change of coordinates  $F : \Omega \rightarrow \tilde{\Omega}$  from the original space to the arrival space. The partial derivative is denoted by

$$F_{I,i} = \frac{\partial X_I}{\partial x_i} \quad \text{for } I, i \in \{1, 2\}.$$

For shortness of notation, we denote the associated (Jacobian) matrix by  $\mathbf{J}$ , which is sometimes referred to as the deformation gradient in this context.

### 3.1. Change of coordinates of plate–shallow-water system

Applying the change of coordinates to the variational formulation (14) gives the following variational form

$$\begin{aligned} \delta \mathbf{S}(\delta \Psi, \Phi, \eta, \delta \eta) = & \int_{t_0}^{t_1} \left[ \int_{\tilde{\Omega}} |\mathbf{J}|^{-1} \rho_w \Psi (\delta \Phi) \left( \eta_{,t} + |\mathbf{J}| \nabla_X \cdot \left( \tilde{\mathbf{H}} \nabla_X \Phi \right) \right) - \delta \eta |\mathbf{J}|^{-1} (\rho_w \partial_t \Phi + \rho_w g \eta + \langle \rho_0, \mathbf{P} \rangle \eta_{,tt}) - \tilde{D}(\delta \eta, \eta) \right] dX_1 dX_2 \\ & + \tilde{BC} - \int_{\partial \tilde{\Omega}} |\mathbf{J}|^{-1} \rho_w \delta \Phi (\mathbf{J}^T \nabla_X \Phi \cdot \mathbf{n}) \Big] dt, \end{aligned} \quad (17)$$

where  $|\mathbf{J}|$  denotes the determinant of  $\mathbf{J}$ ,  $\nabla_X$  is the gradient in the arrival space coordinates  $(X_1, X_2) \in \tilde{\Omega}$  and  $\tilde{\mathbf{H}} = \mathbf{H} \mathbf{J}^T / |\mathbf{J}|$ . The terms  $\tilde{D}$  and  $\tilde{BC}$  are the result of the change of coordinate of the elastic response written as an inner product associated to the tensor  $\mathbf{D}$  with entries  $D_{ijkl}$ , such that

$$\mathbf{D}_{\mathbf{D}}(\epsilon_x(u), \epsilon_x(v)) := u_{,ij} D_{ijkl} v_{,kl}, \quad (18)$$

with  $\epsilon_x$  the symmetrised second-order derivative for the system of coordinate  $x$ , i.e.

$$\epsilon_x(u) = \frac{1}{2} \nabla_x \nabla_x u + \frac{1}{2} (\nabla_x \nabla_x u)^T = \begin{pmatrix} u_{,11} & u_{,12} \\ u_{,12} & u_{,22} \end{pmatrix}.$$

The expressions for  $\tilde{D}$  and  $\tilde{BC}$  are detailed in (20a) below and they generally describe an anisotropic material. Because the determinant of the Jacobian appears in the term containing  $\tilde{\mathbf{H}}$  in (17), the shallow-water equation is shape-invariant only if  $|\mathbf{J}|$  is constant. This point is a well-known aspect of the space transformation method in the shallow-water context; [11] propose a specific change of coordinates for which  $|\mathbf{J}|$  is constant. With this specific change of coordinates, all terms turn out to be shape-invariant except for the elastic part and the water height  $\tilde{\mathbf{H}}$  in the arrival space is anisotropic.

As a result of the coupling of two physical systems, water and plate, the anisotropy involved in the change of coordinates appears in two parameters: the rigidity and the water height. If we want to avoid the design of a non-constant water bed, we must suppose a plate with anisotropic rigidity and immersion. The question of the design of such a plate via effective medium theory has been studied, see e.g. [46], and we do not discuss it here. Therefore, we make use of anisotropic rigidity and immersion in what follows. The elastic response is known not to be shape-invariant in general [23] and we recall the reasons in Section 3.2, making explicit the transformed version of (18) in particular. Indeed, the change of coordinates produces an equation with an extra term, which represents a pre-stress force. This gives rise to two possibilities of how to proceed. The first is to consider the plate with a pre-stress force (as e.g. in [47]); the second is to try to determine plate parameters for which the pre-stress vanishes. This second approach has recently been employed in [30], in which the authors, for a fixed change of coordinates, find specific plate parameters which allow the terms related to the pre-stress to become asymptotically small far from the cylinder. We generalise this approach in Section 3.3 by determining for every change of coordinates the plate parameters that make the pre-stress force term vanish.

### 3.2. Kirchhoff–Love plate equation is not shape-invariant in general

It is well-known that the elastic plate equation is not shape-invariant in general. This is also true for more general waves propagating in elastic media [23–25]. Its invariant form appears with additional terms resulting from the change of coordinate computation. Physically, these additional terms can be seen as an external force. Here, we detail their expression and derive the general boundary conditions resulting from this coordinate change.

With  $\tilde{\Omega}$  being the space in which we will have the cloaking zone (the arrival physical space), the plate rigidity tensor  $D_{IJKL}$  will be computed depending on the rigidity tensor of the plate in the space  $\Omega$  noted  $D_{ijkl}$  where there is no cloak (the original physical space). Considering this notation, we have

$$w_{,ij} = F_{I,i} F_{J,j} W_{,IJ} + F_{I,ij} W_{,I}. \quad (19)$$

Applying the change of coordinate to the elastic term in the plate equation gives

$$\int_{\tilde{\Omega}} \delta w_{,ij} D_{ijkl} w_{,kl} = \int_{\Omega} \mathbf{D}_{\mathbf{D}}(\epsilon_x(\delta w), \epsilon_x(w)) = \int_{\tilde{\Omega}} \tilde{D}(\delta W, W) \quad (20a)$$

$$:= \int_{\tilde{\Omega}} \delta W_{,IJ} \tilde{D}_{IJKL} W_{,KL} + \delta W_{,IJ} \tilde{b}_{IJ}^K W_{,K} + \delta W_{,I} \tilde{b}_{KL}^I W_{,KL} + \delta W_{,I} \tilde{c}_{IK} W_{,K} \quad (20b)$$

with

$$\tilde{D}_{IJKL} = F_{I,i} F_{J,j} F_{K,k} F_{L,l} D_{ijkl} |\mathbf{J}|^{-1}, \quad (21a)$$

$$\tilde{b}_{IJ}^K = F_{I,i} F_{J,j} F_{K,kl} D_{ijkl} |\mathbf{J}|^{-1}, \quad (21b)$$

$$\tilde{c}_{IK} = F_{I,ij} F_{K,kl} D_{ijkl} |\mathbf{J}|^{-1}. \quad (21c)$$

Integration by parts gives the formulation of the elastic response in the arrival space  $\tilde{\Omega}$  as

$$\int_{\tilde{\Omega}} \tilde{D}(\delta W, W) = \int_{\tilde{\Omega}} \delta W (M_{IJ,IJ} - N_{IJ} W_{,IJ} + S_I W_{,I}) + \tilde{B}\tilde{C}(\delta W, W) \quad (22a)$$

$$\tilde{B}\tilde{C}(\delta W, W) = \int_{\partial\tilde{\Omega}} \left( \mathbf{n}^T \begin{pmatrix} Q_{11} & Q_{12} \\ Q_{12} & Q_{22} \end{pmatrix} \mathbf{n} \right) (\nabla \delta W \cdot \mathbf{n}) - \delta W \left[ \begin{pmatrix} Q_{11,1} + Q_{12,2} - R_1 \\ Q_{12,1} + Q_{22,2} - R_2 \end{pmatrix} \cdot \mathbf{n} + \nabla \left( \mathbf{s}^T \begin{pmatrix} Q_{11} & Q_{12} \\ Q_{12} & Q_{22} \end{pmatrix} \mathbf{n} \right) \cdot \mathbf{s} \right] \quad (22b)$$

with  $Q_{IJ} = M_{IJ} + b_{IJ}^K W_{,K}$  and  $R_I = b_{KL}^I W_{,KL} + c_{IK} W_{,K}$ . The term  $M_{IJ,IJ}$  corresponds to the shape-invariant part of the equation, i.e.

$$M_{IJ} = D_{IJKL} W_{,KL} \quad \text{and} \quad M_{IJ,IJ} = (D_{IJKL} W_{,KL})_{,IJ}.$$

The terms  $N_{IJ}$  and  $S_I$  are given by

$$N_{IJ} = -2b_{JK,K}^I + b_{IJ,K}^K + c_{IJ},$$

$$S_I = b_{JK,JK}^I - c_{IJ,J}.$$

Details of the computations to obtain (22) are given in Appendix A. Note that if  $b_{IJ}^K$  and  $c_{IJ}$  vanish, then (22b) has the same form as (5).

In general, the term  $-N_{IJ} W_{,IJ} + S_I W_{,I}$  restricts Eq. (20a) from being invariant. To be shape-invariant, we must allow only coordinate changes satisfying  $-N_{IJ} W_{,IJ} + S_I W_{,I} = 0$ . As explained in [31], because  $N_{IJ}$  and  $S_I$  are factors of Hessian terms (i.e. depend on the second derivative of the transformation), they vanish for linear transformations, which thus leads to a shape-invariant equation and, in turn, perfect cloaking. From the physical point of view, the term  $-N_{IJ} W_{,IJ} + S_I W_{,I}$  corresponds to a pre-stress term and an internal force. We aim to avoid this when we add the part arising from the water to the considerations.

### 3.3. How to choose plate parameters to have a shape-invariant equation

To control the parameters that give the pre-stress force, we can write the plate parameters in the arrival space in terms of the change of coordinate  $F$  and its derivative. More precisely, we write the plate parameters in the arrival space  $\tilde{D}_{IJKL}$  and the ‘‘error terms’’  $\tilde{b}_{IJ}^K$  and  $\tilde{c}_{IK}$  as solutions of linear operators on initial parameters  $D_{ijkl}$  that depend on  $F$  and its derivative. With these tools, we will show general properties of the change of coordinate applied to the plate equation. In particular, for each change of coordinate  $F$ , we give a class of specific plates such that the corresponding plate equation is shape-invariant.

Let us first rewrite the change of coordinate (19) using the short-hand notation

$$\mathcal{H} \cdot \begin{pmatrix} w_1 \\ w_2 \end{pmatrix} = \mathbf{H}_1 w_1 + \mathbf{H}_2 w_2 \quad \text{for a vector} \quad \begin{pmatrix} w_1 \\ w_2 \end{pmatrix} \quad (23)$$

with  $\mathbf{H}_i \in \mathbb{R}^{2 \times 2}$  the Hessian matrix of  $F_i$  and  $w_i \in \mathbb{R}$ .

Then, in the arrival space, we have

$$\tilde{D}(\delta W, W) = |\mathbf{J}|^{-1} D_{\mathbf{D}} \left( \mathbf{J}^T e_X(\delta W) \mathbf{J} + \mathcal{H} \cdot \nabla_X \delta W, \mathbf{J}^T e_X(W) \mathbf{J} + \mathcal{H} \cdot \nabla_X W \right),$$

where  $D_{\mathbf{D}}(\cdot, \cdot)$  is the inner product associated with the 4th-order symmetric tensor  $\mathbf{D}$  with entries  $D_{ijkl}$ , i.e.

$$D_{\mathbf{D}}(\mathbf{U}, \mathbf{V}) = U_{ij} D_{ijkl} V_{kl}, \quad (24)$$

where  $\mathbf{U}, \mathbf{V} \in \mathbb{R}^{2 \times 2}$ . As shown by (20) and (21), by applying the change of coordinate to the elastic response,  $\tilde{D}$  is decomposed in terms describing the elastic energy of an anisotropic plate and terms describing the action of the pre-stress force. The expression (21) can be seen as linear operators on the entries  $D_{ijkl}$  of the symmetric tensors  $\mathbf{D}$ . We propose to generalise this approach by defining three linear operator on the set of 4th-order symmetric tensor. To aid the manipulation of the equations, we use the Voigt notation.

**Definition 3.1 (Voigt Notation and Tensor Space).** We first introduce the sets  $\mathbb{A}$  and  $\mathbb{S}_n$ , which are the set of all mappings from  $\Omega$  to  $\mathbb{R}$  and the set of all  $n$ th-order symmetric tensors with entries in  $\mathbb{A}$ , respectively. We use the Voigt convention by introducing the symbol  $\hat{\cdot}$  such that:

- For  $\mathbf{U} \in \mathbb{A}^{2 \times 2}$

$$\widehat{\mathbf{U}} = \begin{pmatrix} U_{11} & U_{12} \\ U_{21} & U_{22} \end{pmatrix} = \begin{pmatrix} U_{11} \\ U_{22} \\ \sqrt{2}U_{12} \end{pmatrix}.$$

- For  $\mathbf{D} \in \mathbb{S}_4$

$$\widehat{\mathbf{D}} = \begin{pmatrix} D_{1111} & D_{1122} & \sqrt{2}D_{1112} \\ D_{1122} & D_{2222} & \sqrt{2}D_{2221} \\ \sqrt{2}D_{1112} & \sqrt{2}D_{2221} & 2D_{1212} \end{pmatrix}. \tag{25}$$

With this notation and the definition of  $D_{\mathbf{D}}$  given by (24), we note that  $D_{\mathbf{D}}(\mathbf{U}, \mathbf{V}) = \widehat{\mathbf{U}}^T \widehat{\mathbf{D}} \widehat{\mathbf{V}}$  for  $\mathbf{U}, \mathbf{V} \in \mathbb{A}^{2 \times 2}$ .

We define the following subsets of  $\mathbb{S}_4$ :

- $\mathbb{G} \subset \mathbb{S}_4$  the set of 4th-order symmetric tensors  $\mathbf{G}$ , such that

$$\mathbb{G} := \left\{ \mathbf{G} \in \mathbb{S}_4 \mid \exists \mathbf{g} \in \mathbb{A}^3 : \widehat{\mathbf{G}} = \mathbf{g}\mathbf{g}^T \right\}. \tag{26}$$

Note that  $D_{\mathbf{G}}$  with  $\mathbf{G} \in \mathbb{G}$  is positive and

$$D_{\mathbf{G}}(\mathbf{U}, \mathbf{U}) = \left( g_1 U_{11} + g_2 U_{22} + \sqrt{2}g_3 U_{12} \right)^2, \tag{27}$$

so that there are possible points of degeneracy.

- $\mathbb{S}_{4,\text{ortho}} \subset \mathbb{S}_4$ , the set of 4th-order symmetric tensors given by

$$\mathbb{S}_{4,\text{ortho}} := \left\{ \begin{array}{l} \mathbf{D} \in \mathbb{S}_4 \mid \exists D_{1111}, D_{1122}, D_{2222}, D_{1212} \in \mathbb{A} \text{ and not null :} \\ \widehat{\mathbf{D}} = \begin{pmatrix} D_{1111} & D_{1122} & 0 \\ D_{1122} & D_{2222} & 0 \\ 0 & 0 & 2D_{1212} \end{pmatrix} \end{array} \right\}. \tag{28}$$

- $\mathbb{S}_{4,\text{iso}} \subset \mathbb{S}_4$ , the set of 4th-order symmetric tensors given by

$$\mathbb{S}_{4,\text{iso}} := \left\{ \begin{array}{l} \mathbf{D} \in \mathbb{S}_4 \mid \exists D > 0 \text{ and } 0 < \nu < 1 : \\ \widehat{\mathbf{D}} = \begin{pmatrix} D & \nu D & 0 \\ \nu D & D & 0 \\ 0 & 0 & (1 - \nu)D \end{pmatrix} \end{array} \right\}. \tag{29}$$

**Definition 3.2** (Definition of Linear Operators  $\mathcal{A}$ ,  $\mathcal{B}$ ,  $\mathcal{C}$ ). We define three linear operators acting on  $\mathbb{S}_4$ :

- $\mathcal{A}$  given by

$$D_{\mathcal{AD}}(\mathbf{U}, \mathbf{V}) = D_{\mathbf{D}}(\mathbf{J}^T \mathbf{U} \mathbf{J}, \mathbf{J}^T \mathbf{V} \mathbf{J}) = \widehat{\mathbf{J}^T \mathbf{U} \mathbf{J}}^T \widehat{\mathbf{D}} \widehat{\mathbf{J}^T \mathbf{V} \mathbf{J}}. \tag{30a}$$

- $\mathcal{B}$  given by

$$D_{\mathcal{BD}}(\mathbf{U}, \mathbf{v}) = D_{\mathbf{D}}(\mathbf{J}^T \mathbf{U} \mathbf{J}, \mathcal{H} \cdot \mathbf{v}) = \widehat{\mathbf{J}^T \mathbf{U} \mathbf{J}}^T \widehat{\mathbf{D}} \widehat{\mathcal{H} \cdot \mathbf{v}}. \tag{30b}$$

- $\mathcal{C}$  given by

$$D_{\mathcal{CD}}(\mathbf{u}, \mathbf{v}) = D_{\mathbf{D}}(\mathcal{H} \cdot \mathbf{u}, \mathcal{H} \cdot \mathbf{v}) = \widehat{\mathcal{H} \cdot \mathbf{u}}^T \widehat{\mathbf{D}} \widehat{\mathcal{H} \cdot \mathbf{v}}. \tag{30c}$$

Using these operators,  $\widetilde{D}$  is expressed as

$$\begin{aligned} \widetilde{D}(\delta W, W) &= |\mathbf{J}|^{-1} D_{\mathcal{AD}}(\epsilon_X(\delta W), \epsilon_X(W)) + |\mathbf{J}|^{-1} D_{\mathcal{BD}}(\epsilon_X(\delta W), \nabla_X W) \\ &\quad + |\mathbf{J}|^{-1} D_{\mathcal{BD}}(\epsilon_X(W), \nabla_X \delta W) + |\mathbf{J}|^{-1} D_{\mathcal{CD}}(\nabla_X \delta W, \nabla_X W). \end{aligned}$$

The operator  $\mathcal{A}$  gives the properties of the plate in the arrival space. The operators  $\mathcal{B}$  and  $\mathcal{C}$  give the properties of the force resulting from the change of coordinate. The space  $\mathbb{S}_{4,\text{ortho}}$  is the set of 4th-order tensors representing the rigidity tensor of an orthotropic plate. In the same way,  $\mathbb{S}_{4,\text{iso}}$  is the set of 4th-order tensors representing the rigidity tensor of an isotropic plate. Using the different properties of operators  $\mathcal{A}$ ,  $\mathcal{B}$  and  $\mathcal{C}$ , we will deduce the properties of the plate in the arrival space  $\widetilde{\Omega}$ .

**Proposition 3.3** (Properties of Operator  $\mathcal{A}$ ). The operator  $\mathcal{A}$  has the following properties:

1. By definition,  $\mathcal{A} : \mathbb{S}_4 \rightarrow \mathbb{S}_4$ , and

$$\widehat{\mathcal{A}\mathbf{D}} = \widehat{\mathcal{J}}^T \widehat{\mathbf{D}} \widehat{\mathcal{J}}, \tag{31}$$

where  $\widehat{\mathcal{J}}$  is a non-symmetric  $3 \times 3$ -matrix depending on  $\mathbf{J}$ . It is defined in Appendix B.

2. If  $|\mathbf{J}| \neq 0$ ,  $\mathcal{A}$  is an automorphism on  $\mathbb{S}_4$  ( $\mathbb{A}\mathbb{S}_4 = \mathbb{S}_4$  and  $\mathcal{A}$  is invertible). Moreover,

$$D_{\mathcal{A}^{-1}\mathbf{D}}(\mathbf{U}, \mathbf{V}) = D_{\mathbf{D}}(\mathbf{J}^{-T}\mathbf{U}\mathbf{J}^{-1}, \mathbf{J}^{-T}\mathbf{V}\mathbf{J}^{-1}). \tag{32}$$

3. If  $|\mathbf{J}| \neq 0$ ,  $\mathcal{A}$  is an automorphism on  $\mathbb{G}$  ( $\mathbb{A}\mathbb{G} = \mathbb{G}$  and  $\mathcal{A}$  is invertible). In particular, if  $\mathbf{D} \in \mathbb{G}$  such that  $\widehat{\mathbf{D}} = \widehat{\mathbf{G}}\widehat{\mathbf{G}}^T$  for a  $\mathbf{G} \in \mathbb{A}^{2 \times 2}$  then  $\widehat{\mathcal{A}\mathbf{D}} \in \mathbb{G}$  such that

$$\widehat{\mathcal{A}\mathbf{D}} = \widehat{\mathbf{J}\mathbf{G}\mathbf{J}^T\mathbf{J}\mathbf{G}\mathbf{J}^T}. \tag{33}$$

4.  $\mathbb{A}\mathbb{S}_{4,\text{iso}} \subset \mathbb{S}_{4,\text{ortho}}$  if and only if  $F_{1,1}F_{2,1} + F_{1,2}F_{2,2} = 0$ . (As an example, the transformation to the cylindrical coordinate system satisfies this condition, another possibility is to have  $F_{2,1} = F_{1,2} = 0$ , i.e.  $X_i$  depends only on  $x_i$ .)

5.  $\mathbb{A}\mathbb{S}_{4,\text{iso}} \subset \mathbb{S}_{4,\text{iso}}$  if and only if  $F_{1,1}F_{2,1} + F_{1,2}F_{2,2} = 0$  and  $F_{1,1}^2 + F_{1,2}^2 = F_{2,2}^2 + F_{2,1}^2 = |\mathbf{J}|^2$ . (As an example, every linear transformation  $F$  satisfies these hypotheses.)

**Proof.** 1. Let us define  $\widehat{\mathcal{J}}$ , the non-symmetric  $3 \times 3$ -matrix such that  $\widehat{\mathbf{J}^T\mathbf{U}\mathbf{J}} = \widehat{\mathcal{J}}^T\widehat{\mathbf{U}}$  for all  $\mathbf{U} \in \mathbb{R}^{2 \times 2}$ . Then, by definition

$$D_{\mathcal{A}\mathbf{D}}(\mathbf{U}, \mathbf{V}) = \widehat{\mathbf{J}^T\mathbf{U}\mathbf{J}}^T \widehat{\mathbf{D}} \widehat{\mathbf{J}^T\mathbf{V}\mathbf{J}} = \widehat{\mathbf{U}}^T \widehat{\mathcal{J}}^T \widehat{\mathbf{D}} \widehat{\mathcal{J}} \widehat{\mathbf{V}}.$$

2. With the definition of  $\mathcal{A}^{-1}$  given by (32), we can easily check that

$$\mathcal{A}\mathcal{A}^{-1}\mathbf{D} = \mathcal{A}^{-1}\mathcal{A}\mathbf{D} = \mathbf{D}.$$

3. If  $\mathbf{D} \in \mathbb{G}$  such that  $\widehat{\mathbf{D}} = \widehat{\mathbf{G}}\widehat{\mathbf{G}}^T$ , we have

$$D_{\mathcal{A}\mathbf{D}}(\mathbf{U}, \mathbf{V}) = \widehat{\mathbf{J}^T\mathbf{U}\mathbf{J}}^T \widehat{\mathbf{G}}\widehat{\mathbf{G}}^T \widehat{\mathbf{J}^T\mathbf{V}\mathbf{J}} = \widehat{\mathbf{U}}^T \widehat{\mathcal{J}}^T \widehat{\mathbf{G}}\widehat{\mathbf{G}}^T \widehat{\mathcal{J}} \widehat{\mathbf{V}} = \widehat{\mathbf{U}}^T \widehat{\mathbf{J}\mathbf{G}\mathbf{J}^T\mathbf{J}\mathbf{G}\mathbf{J}^T} \widehat{\mathbf{V}}.$$

4. and 5. Suppose  $\mathbf{D} \in \mathbb{S}_{4,\text{iso}}$ , then

$$\widehat{\mathbf{D}} = \nu D \begin{pmatrix} 1 \\ 1 \\ 0 \end{pmatrix} \begin{pmatrix} 1 & 1 & 0 \end{pmatrix} + D(1-\nu)\mathbf{I}_3, \\ \widehat{\mathcal{A}\mathbf{D}} = \nu D \widehat{\mathbf{J}\mathbf{J}^T\mathbf{J}\mathbf{J}^T} + D(1-\nu)\widehat{\mathcal{J}}^T \widehat{\mathcal{J}}.$$

We deduce from the expressions of  $\widehat{\mathcal{J}}$  and  $\mathbf{J}\mathbf{J}^T$  that  $D_{1112} = D_{2221} = 0$  and  $D_{1111}, D_{1122}, D_{2222}, D_{1212} \neq 0$  if and only if  $F_{1,1}F_{2,1} + F_{1,2}F_{2,2} = 0$ . In the same way, we obtain the condition to have  $\mathcal{A}\mathbf{D} \in \mathbb{S}_{4,\text{iso}}$ .

**Proposition 3.4** (Kernel of  $B$  and  $C$ ). *The kernel of the operators  $B$  and  $C$  is non-empty. If  $F$  is affine then  $\ker(B) \cap \ker(C) = \mathbb{S}_4$ . Otherwise,  $\ker(B) \cap \ker(C) \subset \mathbb{G}$ . We describe two cases depending on  $\Gamma := \widehat{\mathbf{H}}_1 \wedge \widehat{\mathbf{H}}_2 \in \mathbb{A}^3$  (where  $\wedge$  denotes the cross product):*

• If  $\Gamma \neq 0$  then

$$\ker(B) \cap \ker(C) = \left\{ \mathbf{D} \in \mathbb{G} \mid \forall c \in \mathbb{A} : \widehat{\mathbf{D}} = c\Gamma\Gamma^T \right\}. \tag{34}$$

• If  $\Gamma = 0$  then

$$\ker(B) \cap \ker(C) = \left\{ \mathbf{D} \in \mathbb{G} \mid \forall c \in \mathbb{A} \forall \mathbf{g} \in \left(\text{Span}(\widehat{\mathbf{H}}_1)\right)^\perp : \widehat{\mathbf{D}} = c\mathbf{g}\mathbf{g}^T \right\}. \tag{35}$$

Note that the kernel space is one dimensional in the first case, and is a two-dimensional space in the second case.

**Proof.** From definition (30b) and from the definition of  $\mathcal{H}$ , it is clear that if  $\widehat{\mathbf{D}}\widehat{\mathbf{H}}_i = 0$  for  $i \in \{1, 2\}$  then  $\mathbf{D}\mathbf{D}$  and  $\mathbf{C}\mathbf{D}$  are null tensors. Then, for every  $\mathbf{g} \perp \widehat{\mathbf{H}}_1$  and  $\mathbf{g} \perp \widehat{\mathbf{H}}_2$ , taking  $\widehat{\mathbf{D}} = c\mathbf{g}\mathbf{g}^T$  for any  $c \in \mathbb{A}$  will give  $\mathbf{B}\mathbf{D} = 0$  and  $\mathbf{C}\mathbf{D} = 0$ . Because  $\widehat{\mathbf{D}}$  is symmetric this is the only possibility to have both  $\mathbf{B}\mathbf{D} = 0$  and  $\mathbf{C}\mathbf{D} = 0$ .

**Property 3.5** (Invariant Plate Parameters). *For a given coordinate change  $F$  such that  $|\mathbf{J}| \neq 0$ , choosing a plate in the original space  $\Omega$  with rigidity tensor  $\mathbf{D} \in \ker(B) \cap \ker(C)$  given by Proposition 3.4 will ensure the plate equation is shape-invariant for this transformation. The obtained rigidity operator  $\widetilde{\mathbf{D}}$  in the arrival space  $\widetilde{\Omega}$  is given by  $\widetilde{\mathbf{D}} = |\mathbf{J}|^{-1}D_{\mathcal{A}\mathbf{D}}$ .*

*Application of the space transformation method for a plate.* The operator  $A$  defines the parameters of the plate in the arrival space. The operators  $B$  and  $C$  define the pre-stress force obtained after the change of coordinates. In most works, the change of coordinates for cloaking an object is applied to an isotropic material. In this case, [Proposition 3.3](#) gives conditions on the change of coordinates  $F$  to ensure that the image of the isotropic plate is orthotropic (and not fully anisotropic). We see that possible changes of coordinates to obtain such result are restrictive. Moreover, for changes of coordinates mostly used in cloaking (e.g. inflating a point), the image of an isotropic plate (subject to free boundary conditions) is not orthotropic.

In the context of cloaking, most considered changes of coordinates  $F$  have non-vanishing  $\Gamma$ . [Property 3.5](#) gives plate parameters that ensure no pre-stress force after the change of coordinates  $F$ . This means that, for every transformation  $F$  such that  $\Gamma := \widehat{\mathbf{H}}_1 \wedge \widehat{\mathbf{H}}_2 \neq 0$  (where  $\wedge$  denotes the cross product), there exists a class of plates whose rigidity tensors  $\mathbf{D}$  are in  $\ker(B) \cap \ker(C)$ , such that the elastic energy is shape-invariant with respect to the transformation  $F$ . More precisely, taking  $\widehat{\mathbf{D}} = c(x_1, x_2) \Gamma \Gamma^T$  for any mapping  $c : \Omega \rightarrow \mathbb{R}$ , the obtained rigidity tensor  $\mathcal{A}\mathbf{D}$  in the arrival space  $\widetilde{\Omega}$  is given by its Voigt representation  $\widehat{\mathcal{A}\mathbf{D}} = |\mathbf{J}|^{-1} c(x_1, x_2) \mathbf{g}\mathbf{g}^T$  with  $\mathbf{g} = \widehat{\mathbf{J}\mathbf{G}\mathbf{J}^T}$  where  $\widehat{\mathbf{G}} = \Gamma$ . Note that both plate parameters (in the original space  $\Omega$  and the arrival space  $\widetilde{\Omega}$ ) are in the set  $\mathbb{G}$  defined in [Definition 3.1](#) that ensure by (27) that the elastic energy of the plate is positive if  $c$  is positive.

**Property 3.6 (Shape-Invariant Coupled Plate–Water Equation).** *Suppose a change of coordinate  $F$  with its Jacobian matrix  $\mathbf{J}$  such that  $|\mathbf{J}|$  is constant. Then, for any plate parameters represented by the tensor  $\mathbf{D} \in \ker(B) \cap \ker(C)$ , the floating-plate system (15) is shape-invariant for the transformation  $F$ .*

**Proof.** From the variational form (17), because  $|\mathbf{J}|$  is constant, the water height can be taken as  $\mathbf{H}' = \mathbf{J}^T \mathbf{H}\mathbf{J}$  and the transformed  $\eta$  describes the surface elevation in the arrival space. Also, by [Property 3.6](#), the elasticity term is shape-invariant and

$$\widetilde{\mathcal{D}}(\delta\eta, \eta) = (|\mathbf{J}|^{-1} \delta\eta)_{,IJ} |\mathbf{J}| D_{IJKL}(\eta)_{,KL} = \mathcal{D}_{\mathcal{A}\mathbf{D}}(|\mathbf{J}|^{-1} \epsilon_X(\delta\eta), \epsilon_X(\eta)).$$

Injecting the above into the variational form (17) gives

$$\begin{aligned} \delta\mathbf{S}(\delta\boldsymbol{\Psi}, \boldsymbol{\Phi}, \eta, \delta\eta) &= \int_{t_1}^{t_2} \left[ \int_{\widetilde{\Omega}} |\mathbf{J}|^{-1} \rho_w \boldsymbol{\Psi}(\delta\boldsymbol{\Phi}) (\eta_{,t} + \nabla_X \cdot (\mathbf{H}' \nabla_X \boldsymbol{\Phi})) \, dX_1 dX_2 \right. \\ &\quad - \int_{\widetilde{\Omega}} \delta\eta |\mathbf{J}|^{-1} (\rho_w \partial_t \boldsymbol{\Phi} + \rho_w \mathbf{g}\eta + \langle \rho_0, \mathbf{P} \rangle \eta_{,tt} + (|\mathbf{J}| D_{IJKL} \eta_{,KL})_{,IJ}) \, dX_1 dX_2 \\ &\quad \left. - \int_{\partial\widetilde{\Omega}} |\mathbf{J}|^{-1} \rho_w \delta\boldsymbol{\Phi} (\mathbf{J}^T \nabla_X \boldsymbol{\Phi} \cdot \mathbf{n}) + \widetilde{\mathcal{B}\mathcal{C}} \right] dt. \end{aligned}$$

Therefore, the plate rigidity matrix in the arrival space is given by  $\widehat{\mathcal{A}\mathbf{D}}$ .

#### 4. Application of the space transformation method to the floating plate

In this section, we give an example how the space transformation method can be applied to a floating plate. For this purpose, we consider a transformation within the scope of [Property 3.6](#), and which results in a shape-invariant system. We show how this transformation can be used to cloak a rigid bottom-mounted circular cylinder piercing the water surface. (We briefly discuss the case of cloaking an inner hole of open water (polynya) instead of a vertical cylinder in [Appendix C](#).)

More specifically, we give a transformation  $F$ , which inflates the cylinder and transforms the plate parameters in the vicinity of the cylinder (the cloak region). Thus, we devise plate parameters such that the forcing on the transformed (larger) cylinder is the same as on the original smaller cylinder (similarly to Kohn et al. [48], who considered the blow-up of a small ball to design a cloak decreasing the scattering of Dirichlet inclusions in the context of electric impedance tomography). The geometrical meaning of the transformation scheme is illustrated in [Fig. 2](#).

##### 4.1. Example of a shape-invariant floating plate system

Consider the change of coordinate proposed by [11] for cloaking in shallow water (without plate) written in polar coordinates as  $F(r, \theta) = (\sqrt{\tilde{b}r^2 + \tilde{a}}, \theta)$ , where  $\tilde{a}, \tilde{b} > 0$ , which gives  $|\mathbf{J}| = \tilde{b}$  (i.e. a constant). According to [Section 3.3](#), the system (15) is shape-invariant for this change of coordinate  $F$  (i.e.  $BD = 0$  and  $CD$ ). Thus, the corresponding rigidity tensor in the original space  $\Omega$  is given by

$$\mathcal{D}(\epsilon_x(u), \epsilon_x(v)) = \begin{pmatrix} u_{,11} & u_{,22} & u_{,12} \end{pmatrix} c(x_1, x_2) \begin{pmatrix} \Gamma_1^2 & \Gamma_1 \Gamma_2 & \Gamma_1 \Gamma_3 \\ \Gamma_1 \Gamma_2 & \Gamma_2^2 & \Gamma_2 \Gamma_3 \\ \Gamma_1 \Gamma_3 & \Gamma_2 \Gamma_3 & \Gamma_3^2 \end{pmatrix} \begin{pmatrix} v_{,11} \\ v_{,22} \\ v_{,12} \end{pmatrix} \tag{36}$$

with

$$\begin{aligned} \Gamma_1(r, \theta) &= \tilde{b} (x_1^2 + x_2^2)^2 + \tilde{a} x_1^2, \\ \Gamma_2(r, \theta) &= \tilde{b} (x_1^2 + x_2^2)^2 + \tilde{a} x_2^2, \\ \Gamma_3(r, \theta) &= \tilde{a} x_1 x_2 \end{aligned}$$

and an arbitrary function  $c > 0$ . The parameters of the plate after the change of coordinate  $F$  can be computed by the formula given in [Proposition 3.3](#).

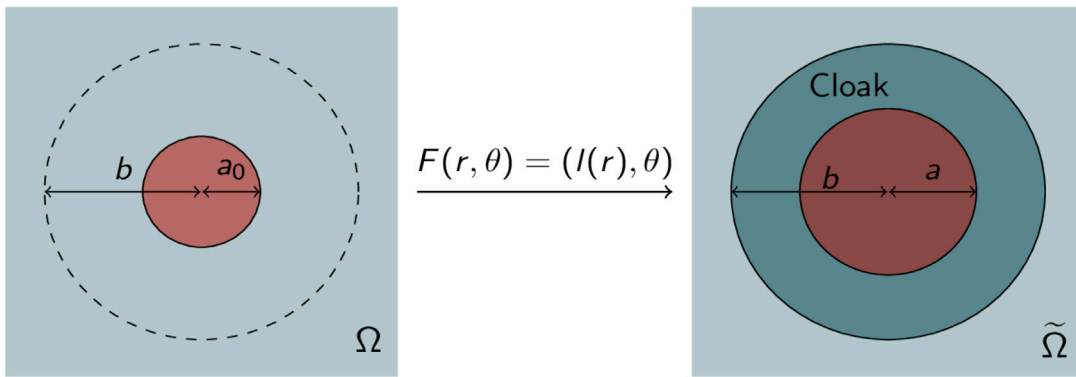


**Fig. 2.** Scheme of the change of coordinate used to compute plate parameters in the cloak zone. In order to determine the cloak of radius  $b$  around the cylinder of radius  $a < b$ , we start from a smaller cylinder of radius  $0 \leq a_0 < a$ , which is then transformed (inflated) to the desired radius  $a$  by means of the transformation  $F$ . The region  $\{(r, \theta, z) \mid r > b\}$  is not affected by the transformation. As the force and scattering in  $\tilde{\Omega}$  is the same as in the untransformed domain  $\Omega$ , it is much smaller than it would be without the cloak. Note that  $a_0 = 0$  is a possible choice.

4.2. Cloaking a rigid bottom-mounted surface-piercing circular cylinder

We consider water of constant depth  $d$  and a rigid bottom-mounted surface-piercing circular cylinder of radius  $a_0$ , so that  $\Omega = \{(x_1, x_2) : x_1^2 + x_2^2 > a_0^2\}$  (see Fig. 1 as well as the left panel of Fig. 2), a rigidity tensor of the plate given by (36) and an immersion  $p$ . We start with  $a_0 > 0$  in order to take care of the boundary conditions in the change of coordinates explicitly (instead of  $a_0 = 0$ , which is often used in the electromagnetism community). Note that Property 3.5 remains valid for the choice  $a_0 = 0$  but the boundary condition would have to be treated separately. The governing equations are given by (15) in the original space. In view of Section 4.1, consider the transformation  $F$  with respect to polar coordinates,  $F(r, \theta) = (l(r), \theta)$ , where

$$l(r) = \begin{cases} \frac{a}{a_0}r, & r < a_0, \\ \sqrt{\frac{b^2 - a^2}{b^2 - a_0^2}r^2 + b^2 \frac{a^2 - a_0^2}{b^2 - a_0^2}}, & a_0 \leq r \leq b, \\ r, & b > r, \end{cases} \tag{37}$$

noting that  $l$  is a bijection. This transformation acts within the cylinder of radius  $b > a_0$  containing the bottom-mounted cylinder of radius  $a_0$  and plate-covered water ( $a_0 < r < b$ ), while leaving the region outside this cylinder invariant. Inside this cylinder, the transformation acts to inflate the cylinder of radius  $a_0$  to radius  $a$ , while the plate-covered water region in the hollow cylinder of inner radius  $a_0$  and outer radius  $b$  is mapped to the cloak region, which is a hollow cylinder of inner radius  $a$  and outer radius  $b$ , see Fig. 2.

The plate properties in  $\tilde{\Omega} = \{(X, Y), a < R(X, Y) < b\}$  of the cloak around the cylinder of radius  $a$  is given by the tensor

$$\tilde{D}(u, v) = |\mathbf{J}| \mathcal{D}_{AD}(\epsilon_X(U), \epsilon_X(V)) \quad \text{with} \quad |\mathbf{J}| = \tilde{b}, \tag{38a}$$

$$\tilde{b} = \frac{b^2 - a^2}{b^2 - a_0^2} \quad \text{and} \quad \tilde{a} = b^2 \frac{a^2 - a_0^2}{b^2 - a_0^2}. \tag{38b}$$

Moreover, the plate immersion is given by the anisotropic expression

$$-\tilde{p}(X_1, X_2) = \mathbf{J}^T H \mathbf{J} - d, \tag{38c}$$

$$\text{where } \mathbf{J} = \left( R^2 r^3 \tilde{b} \right)^{-1} \begin{pmatrix} \Gamma_2^2 + \Gamma_3^2 & -(\Gamma_2 + \Gamma_2) \Gamma_3 \\ -(\Gamma_2 + \Gamma_2) \Gamma_3 & \Gamma_1^2 + \Gamma_2^2 \end{pmatrix} \quad \text{and} \quad r = l^{-1}(R) = \sqrt{\frac{R^2 - b^2(a^2 - a_0^2)}{b^2 - a^2}}.$$

5. Approximate numerical illustration: reduction of the force on and scattering by a bottom-mounted cylinder

In the context of the geometry shown in Figs. 1 and 2, and analogous to Section 4.2, we illustrate the reduction of the wave forcing on the bottom-mounted cylinder by the cloak through a numerical example. In order to keep the computations simple and the system of equations amenable to an eigenfunction matching solution method, we use a transformation with non-constant  $|\mathbf{J}|$ , contrary to Section 4.2, which makes the results approximate only. For the same reason, we take the plate in the untransformed domain to have a simple form of the rigidity tensor, which has a degeneracy with respect to the shear component but the associated rigidity tensor falls within the hypotheses of Property 3.5 and we note that the transformed parameters (the physically relevant parameters of the cloak) turn out not to have this degeneracy in the shear component.

### 5.1. The untransformed geometry

We consider water of constant depth  $d$  and a cylinder of radius  $a_0$  so that  $\Omega = \{(x_1, x_2) : x_1^2 + x_2^2 > a_0\}$ , also see Fig. 1 as well as the left panel of Fig. 2, and a rigidity tensor of the plate, which we assume to have constant immersion  $p$ , to satisfy  $D_{1111} = D_{2222} = D_{1122} =: D > 0$  and  $D_{1112} = D_{2221} = D_{1212} = 0$ , thus given by

$$\mathcal{D}_{\mathbf{D}_0}(\epsilon_x(u), \epsilon_x(v)) = \begin{pmatrix} u_{,11} & u_{,22} & \sqrt{2}u_{,12} \end{pmatrix} \begin{pmatrix} D & D & 0 \\ D & D & 0 \\ 0 & 0 & 0 \end{pmatrix} \begin{pmatrix} v_{,11} \\ v_{,22} \\ \sqrt{2}v_{,12} \end{pmatrix}. \tag{39}$$

Under these assumptions, the governing Eqs. (15) become

$$-\alpha\xi + H\Delta\phi = 0 \quad \text{on } \Omega, \tag{40a}$$

$$-\alpha\rho_w\phi + \rho_w g\xi + D\Delta^2\xi - \rho_0 P\alpha^2\xi = 0 \quad \text{on } \Omega, \tag{40b}$$

$$\nabla\phi \cdot \mathbf{n} = 0 \quad \text{on } \partial\Omega, \tag{40c}$$

$$\partial_r\Delta\xi = \Delta\xi = 0 \quad \text{on } \partial\Omega, \tag{40d}$$

$$\phi - \phi_{\text{inc}} \text{ satisfy radiation condition,} \tag{40e}$$

with constant  $H = d - p$ . We note that this resulting system is the same as that for an isotropic plate but with different boundary conditions (40d).

A solution to this system can be devised by eigenfunction matching. For this purpose, we use (40a) in (40b), which leads to

$$\alpha^2\rho_w\phi + \rho_w gH\Delta\phi + DH\Delta^3\phi - \rho_0 P\alpha^2 H\Delta\phi = 0. \tag{41}$$

Eq. (41) can be factorised as

$$\prod_{i=0}^2 (\Delta - k_i^2)\phi = 0 \quad \text{with } k_i \in \mathbb{C} \quad \text{and } \Im(k_i^2) \geq 0, \tag{42}$$

where the  $k_i$  are solutions of the dispersion relation

$$DHk_i^6 + (\rho_w - \rho PH\alpha^2)k_i^2 + \alpha^2\rho_w = 0.$$

We suppose  $k_0 > 0$  and an incident wave given by  $\xi_{\text{inc}} = A_0 e^{ik_0 x_1}$ , the corresponding potential  $\phi_{\text{inc}}$  is given by (40a) as

$$\phi_{\text{inc}} = \frac{iA_0\alpha}{Hk_0^2} e^{ik_0 x_1}.$$

System (40), noting (42), is now solved using the eigenfunction matching method which is based on expanding the potential, and correspondingly the plate displacement, in cylindrical eigenfunctions as

$$\phi = \phi_{\text{inc}} + \sum_m \sum_{i \in \{0,1,2\}} B_{i,m} H_m^{(1)}(k_i r) e^{im\theta}, \tag{43}$$

$$\xi = \xi_{\text{inc}} + \sum_m \sum_{i \in \{0,1,2\}} C_{i,m} H_m^{(1)}(k_i r) e^{im\theta}, \tag{44}$$

where  $H_m^{(1)}$  is the Hankel function of the first kind of order  $m$ . Injecting (43) into (40c) and (40d) leads to a linear system of equations to be solved for the unknowns  $B_{i,m}$  for each  $m$ . The  $C_{i,m}$  are deduced afterwards using (40a). The details of the application of the method to a floating plate can be found in [37,49].

### 5.2. Force on the cylinder and scattering cross-section

In order to assess the performance of the cloak, we measure the force exerted on the cylinder and the scattering cross-section. The force on a vertical cylinder of radius  $a$  in the  $x_1$ -direction, which is the direction of the incident wave, is given by

$$F(a) = \int_0^{2\pi} \cos(\theta)\phi(a, \theta)d\theta. \tag{45}$$

Moreover, the scattering cross-section, which is a measure for the scattering strength, for a vertical cylinder of radius  $a$  is given by

$$S(a) = \frac{1}{2\pi} \int_0^{2\pi} \left| \frac{\mathcal{A}_0(\theta)}{A_0} \right|^2 d\theta. \tag{46}$$

Here, the diffracted far-field amplitude  $\mathcal{A}_0$  is defined via

$$\xi_D \equiv \xi - \xi_{\text{inc}} \sim \sqrt{\frac{2}{\pi k_0 r}} e^{i(k_0 r - \pi/4)} \mathcal{A}_0 \quad \text{as } r \rightarrow \infty. \tag{47}$$

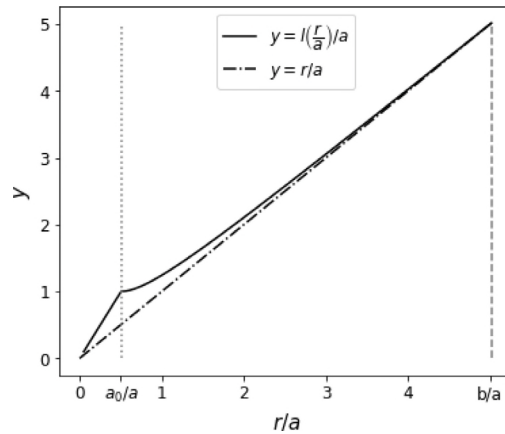


**Fig. 3.** Graph of function  $l$  as a function of the non-dimensional variable  $r/a \in [0, b/a]$  (solid line). Dash-dotted line represents the corresponding identity function ( $y = r/a$ ).

Assuming we have only one propagating mode  $k_0$  and injecting the far-field asymptotics  $H_m^{(1)}(r) \sim \sqrt{\frac{2}{\pi z}} e^{i(k_0 z - m\pi/2 - \pi/4)}$  as  $r \rightarrow \infty$  into (43) gives

$$\mathcal{A}_0(\theta) = \sum_m C_{0,m} e^{im(\theta - \pi/2)}. \tag{48}$$

### 5.3. The transformation

According to Section 3.3, we can define a change of coordinates  $F$  such that the system (40) is shape-invariant for this change of coordinate (i.e.  $BD_0 = CD_0 = 0$ ).

**Property 5.1** (The Change of Coordinates Associated To  $D_0$ ). For every transformation  $F$  with respect to polar coordinates, which is of the form  $F(r, \theta) = (\beta r + \gamma/r, \theta)$ , where  $\gamma, \beta \in \mathbb{R}$ , we have  $BD_0 = CD_0 = 0$ .

Consider the transformation  $F$  with respect to polar coordinates,  $F(r, \theta) = (l(r), \theta)$ , where

$$l(r) = \begin{cases} \frac{a}{a_0} r, & r \leq a_0, \\ (1 - \varepsilon) \left( r + \frac{a_0^2}{r} \right), & a_0 \leq r \leq b, \\ r, & b \leq r, \end{cases} \tag{49a}$$

$$\text{with } a_0 = \frac{a}{2(1 - \varepsilon)} \quad b = \frac{a}{2\sqrt{\varepsilon(1 - \varepsilon)}}, \tag{49b}$$

where  $a, \varepsilon > 0$  are given and  $\varepsilon$  can be chosen such that  $\varepsilon < 1/2$  to ensure that  $l$  is a bijection. Transformation (49) is taken such that there exists a fixed point  $l(b) = b$ ,  $l$  is increasing in  $[a_0, b]$  and  $a = l(a_0) > a_0$ . This choice limits the ratio  $a/a_0$ , such that  $a/a_0 \in ]1, 2[$ . Note that the cloak of radius  $b$  increases when  $\varepsilon$  decreases and  $a/a_0 \rightarrow 2$  as  $\varepsilon \rightarrow 0$ . Moreover, the ratio  $a/a_0$  cannot be increased under these conditions. Fig. 3 represents the function  $f$  for the non-dimensional variable  $r/a \in [0, b/a]$ .

The determinant of the Jacobian is

$$|\mathbf{J}| = \begin{cases} 2(1 - \varepsilon) & r \leq a_0, \\ (1 - \varepsilon)^2 \left( 1 - \frac{a_0^4}{r^4} \right), & a_0 \leq r \leq b, \\ 1 & b \leq r, \end{cases}$$

which is non-constant. By neglecting the variations of  $|\mathbf{J}|$  in the shallow-water equation, the prediction of the cloaking plate parameters in the arrival space  $\tilde{\Omega} = \{(X, Y), a < R(X, Y) < b\}$  is only approximate. The approximation of such plate properties is given by the tensor

$$\tilde{D}_0(u, v) = \begin{pmatrix} u_{,11} & u_{,22} & \sqrt{2}u_{,12} \end{pmatrix} \tilde{D}(R) \begin{pmatrix} G_1^2 & G_1 G_2 & \sqrt{2}G_1 G_3 \\ G_1 G_2 & G_2^2 & \sqrt{2}G_2 G_3 \\ \sqrt{2}G_1 G_3 & \sqrt{2}G_1 G_3 & 2G_3^2 \end{pmatrix} \begin{pmatrix} v_{,11} \\ v_{,22} \\ \sqrt{2}v_{,12} \end{pmatrix} \tag{50a}$$

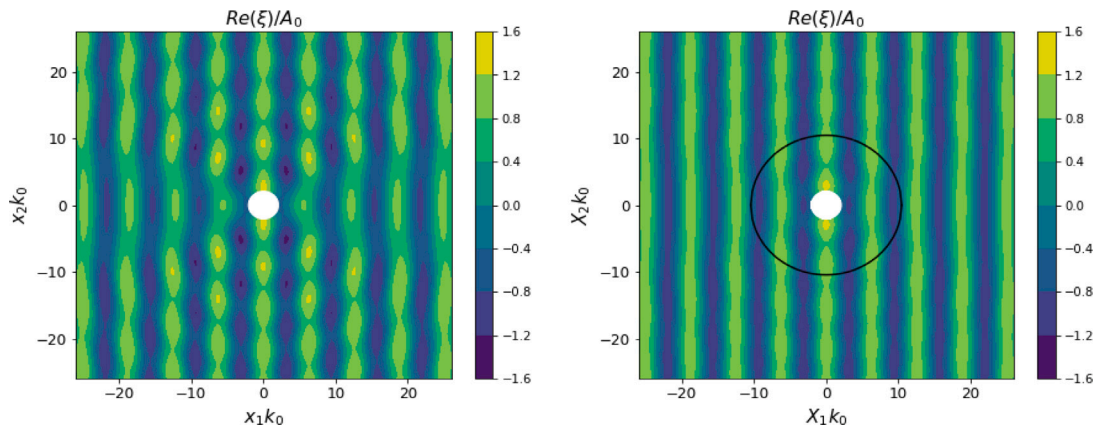


**Fig. 4.** Surface elevation for a wave incident on a bottom-mounted cylinder of radius  $a = 20\text{m} \approx 10/k_0$  from the left for the plate with anisotropic parameters  $(D_0, p)$  everywhere (left panel) and in the case that the plate parameters are  $(\tilde{D}, \tilde{p})$  within the cloak region marked by the black circle (right panel). (Computed using eigenfunction matching method (43), (44) with  $m = 10$ ; axes are given by the non-dimensional variable  $X_i k_0$ ).

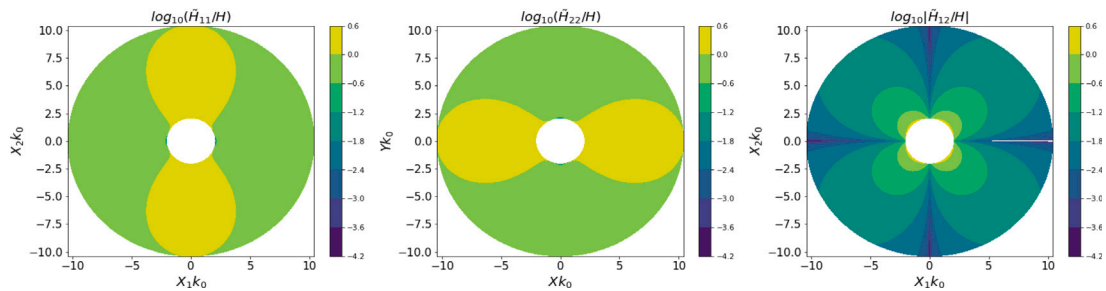


**Fig. 5.** Anisotropic water height  $\tilde{\mathbf{H}}/H$  given by (51) in the cloak with respect to the non-dimensional coordinate  $k_0 X_i$ . The left-hand panel represents  $\tilde{\mathbf{H}}_{11}/H$ , middle panel  $\tilde{\mathbf{H}}_{22}/H$  and right-hand panel  $\tilde{\mathbf{H}}_{12}/H$ .

with

$$\tilde{D}(R) = Dr^{-4}, \quad r = l^{-1}(R) = \frac{R + \sqrt{R^2 - a^2}}{2(1 - \epsilon)}, \tag{50b}$$

$$G_1 = R^2 - a^2 \cos(\theta)^2, \quad G_2 = R^2 - a^2 \sin(\theta)^2, \quad G_3 = -a^2 \cos(\theta) \sin(\theta). \tag{50c}$$

Moreover, the plate immersion is given by the anisotropic expression

$$\tilde{\mathbf{H}}(R) = r^{-2} \begin{pmatrix} G_1 & G_3 \\ G_3 & G_2 \end{pmatrix} \quad \text{and} \quad \tilde{\mathbf{p}} = -\tilde{\mathbf{H}} + d\mathbf{I}_2. \tag{51}$$

### 5.4. Numerical illustration

In order to illustrate the reduction of force and scattering, we compute the solution for the parameters  $H = 5\text{ m}$ ,  $\alpha = 1\text{ s}^{-1}$ ,  $P = 0.05\text{ m}$ ,  $D = 36630\text{ Pa m}^3$  and  $\rho = 500\text{ kg m}^{-3}$ , which are typical parameter values for a polystyrene plate. The water density is taken as that of sea water,  $\rho_w = 1024\text{ kg m}^{-3}$ . This gives a propagating mode outside the cloak region of wavelength  $\lambda = 2\pi/k_0 \approx 60\text{ m}$ . Considering an incident wave of amplitude  $A_0 = 0.5\text{ m}$ , these parameters verify  $P \ll A_0 \ll H \ll \lambda$ .

We begin with a visual illustration of the impact of the cloak. For a bottom-mounted cylinder of radius  $a = 20\text{ m}$  and transformation  $F$  taken with  $\epsilon = 0.01$ , Fig. 4 compares the surface elevation for the plate given by  $(D_0, p)$  everywhere (left panel) to the case where it is chosen as  $(\tilde{D}_0, \tilde{p})$  in the cloak region (right panel). A reduction of the scattering is clearly visible. There is hardly any scattering to the far field in the case including the cloak, which is identical to the scattering by the uncloned cylinder of radius  $a_0$ . The graphs of each element of  $\tilde{\mathbf{H}}$  and  $\mathcal{A}D_0$  corresponding to this example are given in Figs. 5 and 6, respectively.

In order to quantify this, Fig. 7 shows the force exerted on the bottom-mounted vertical cylinder, given by (45), (left panel) and the scattering cross-section, given by (46), (right panel) versus cylinder radius and frequency for three cases. The dashed line shows the results for a plate with rigidity tensor  $(D_0, p)$  everywhere, i.e. without a cloak, and the solid line shows the results for the plate with rigidity tensor  $(\tilde{D}, \tilde{p})$  in the vicinity of the cylinder, i.e. with the cloak. For comparison, we also show the solution for the case

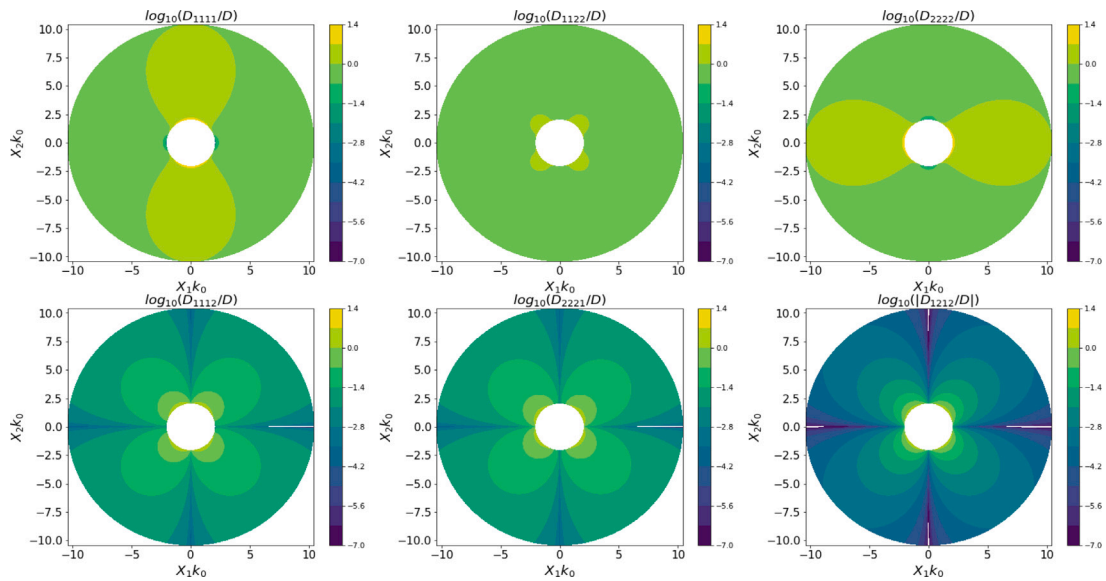


**Fig. 6.** Anisotropic rigidity tensor  $\widehat{\mathbf{AD}}_{ij}/D$  given by (50) in the cloak with respect to the non-dimensional coordinate  $k_0 X_i$ . Upper row:  $\widehat{\mathbf{AD}}_{11}/D$  (left),  $\widehat{\mathbf{AD}}_{22}/D$  (middle),  $\widehat{\mathbf{AD}}_{12}/D$  (right). Bottom row:  $\widehat{\mathbf{AD}}_{13}/D$  (left),  $\widehat{\mathbf{AD}}_{23}/D$  (middle),  $\widehat{\mathbf{AD}}_{33}/D$  (right).

of an isotropic plate with the same rigidity constant (and without a cloak), which is shown as a dotted line and coincides with the results for the anisotropic plate without cloak everywhere. To be precise, for this last case we imposed the same values of flexural rigidity  $D$  and plate thickness  $P$  as before and choose the Poisson’s ratio to be  $\nu = 0.3$ , which corresponds to a Young’s modulus  $E = 3.2 \times 10^9$  Pa and classic free plate boundary condition. For radii up to  $ak_0 \leq 10$ , the force exerted on the vertical cylinder as shown in Fig. 7 (left panel) is reduced for the plate with the cloak compared to the plate without cloak. Up to about  $ak_0 \leq 1$ , the two lines are parallel, implying that the cloak leads to reduction of the force on the cylinder, which is constant in the log–log setting. The same global behaviour is observed for the force for frequencies  $\alpha \sqrt{d/g} < 10^{0.4}$  as shown in the second row of Fig. 7. A similar behaviour is observed for the scattering cross-section in Fig. 7 (right panel), for which a significant reduction is achieved by the cloak for all radii considered.

To illustrate the reduction of the force and the scattering in the case of the plate with the cloak, Fig. 8 shows the evolution of  $F_\epsilon(a)$  (left panel) and  $S_\epsilon(a)$  (right panel) as a function of  $\epsilon$ , which is given by the ratio  $a/a_0 = 2(1 - \epsilon) \in [1, 2[$  for different values of cylinder radius  $a$ . The graphs are normalised by the case  $\epsilon = 1/2$ , which corresponds to the case with plate parameters  $(\mathbf{D}_0, p)$  and no cloak. As can be seen, the force and the scattering is reduced for all values of  $a$ , and more so as  $\epsilon$  becomes smaller. For  $ak_0 \leq 0.5$ , the force is nearly halved by the cloak when  $\epsilon$  is sufficiently small, which confirms the observations made from Fig. 8. A similar behaviour is observed for the scattering cross-section in the right panel.

**6. Conclusion and outlook**

We derived a variational formulation for a fully anisotropic plate floating on shallow water and we extended the change of coordinates method used in the cloaking principle to this situation. We constructed the equations of motion for an anisotropic plate floating on water from variational formulations in each domain. These variational formulations allow us to apply the change of coordinate in the weak formulations and simplify the formulation with respect to the elastic energy part. We recall that, for a general change of coordinates, the elastic energy part is not shape-invariant but produces additional terms that can be interpreted as a pre-stress force. A main purpose of this paper was to treat the terms producing the pre-stress force in its variational form and gave conditions when these terms vanish. In particular, we showed that for each change of coordinate one can find a class of anisotropic plates which are shape-invariant for the particular change of coordinate. Applied to the model of a floating plate, it gives plates with anisotropic rigidity and immersion.

In the context of cloaking, our results extend known methods to anisotropic plates for reducing the force on and scattering due to an object by not restricting the study to an isotropic plate in the original space. The model presented assumes a dual anisotropy in the rigidity and immersion of the plate.

In order to put the results into practice, it remains to study how such a double anisotropy can be realised, possibly based on metamaterials devised via homogenisation. Another potential next step is to consider a floating plate of finite extent and study its boundary effects. A first approach in this direction could be to find the anisotropic plate that achieves no scattering. Then the given tool in this paper would allow to indicate a suitable transformation to apply the space transformation method to this plate and fine-tune the parameters of a plate of finite extent in order to achieve perfect, or at least nearly perfect, cloaking. Extensions to the reduction of scattering by or sloshing within polynyas might also be of interest (see the discussion in Appendix C).

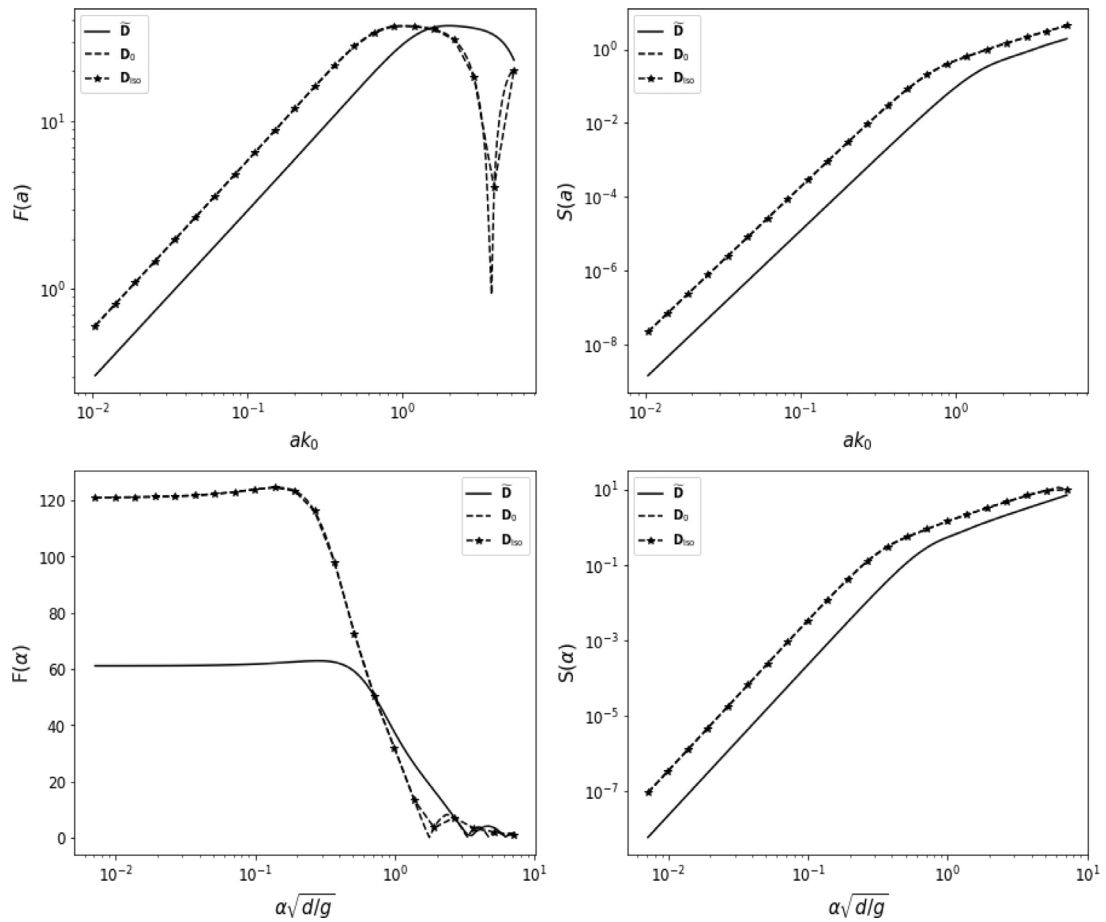


**Fig. 7.** Left panel: Force on vertical cylinder given by (45) versus non-dimensional radius  $ak_0$  (top) and frequency  $\alpha$  (bottom). Right panel: Scattering cross-section as given by (46) versus non-dimensional radius  $k_0a$  (top) and frequency  $\alpha\sqrt{d/g}$  (bottom). For all panels : Solid lines correspond to the plate with parameters  $(\bar{D}, \bar{p})$  inside the cloak region while dashed lines correspond to the plate with parameters  $(D_0, p)$  everywhere, i.e. without the cloak. The starred lines show the results for a corresponding isotropic plate that is superposed to the one corresponding to  $D_0$ .

**CRedit authorship contribution statement**

**Sophie Thery:** Methodology, Investigation, Formal analysis, Software, Visualisation, Writing. **Malte A. Peter:** Conceptualization, Methodology, Writing, Supervision. **Luke G. Bennetts:** Conceptualization, Writing – review. **Sébastien Guenneau:** Conceptualization, Writing – review.

**Declaration of competing interest**

The authors declare that they have no known competing financial interests or personal relationships that could have appeared to influence the work reported in this paper.

**Acknowledgments**

This work was supported by the EU through the H2020-MSCA-RISE-2020 project EffectFact, Grant Agreement ID: 101008140. LGB is funded by an Australian Research Council Future Fellowship (FT190100404). The authors thank the Isaac Newton Institute for Mathematical Sciences, Cambridge, for support and hospitality during the MWS programme where work on this paper was undertaken (supported by EPSRC grant no EP/R014604/1).

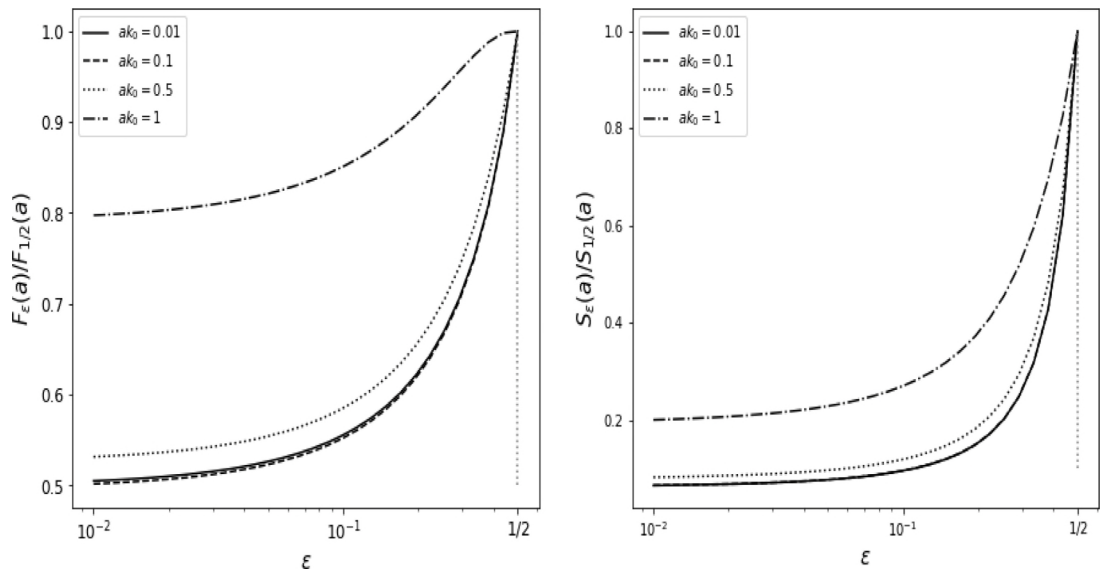


**Fig. 8.** Normalised force on vertical cylinder (45) versus parameter  $\epsilon \in [10^{-2}, 0.5]$  (left) and normalised scattering cross-section as given by (46) versus  $\epsilon$  (right). Both panels: The different lines correspond to different values of the cylinder radius  $a$ . The force  $F_\epsilon(a)$  and the scattering cross-section  $S_\epsilon(a)$  correspond to a plate including a cloaking region around the cylinder given by plate parameters  $(\tilde{D}, \tilde{\rho})$  (see (50)) depending on  $\epsilon$ , which defines the cylinder radius in the untransformed plate ( $a_0 = 2/2(1 - \epsilon)$ ). The limit case  $\epsilon = 1/2$  corresponds to no transformation, i.e.  $a_0 = a = b$  and, thus, no cloak.

**Appendix A. Extraction of general boundary conditions**

Boundary conditions (4) are obtained through two successive integrations by parts on the weak formulation (2). We detail the derivation by focusing on the elastic term in (2):

$$\begin{aligned} \int_{\Omega} \delta w_{,ij} D_{ijkl} w_{,kl} &= \int_{\Omega} \delta w_{,11} M_{11} + \delta w_{,22} M_{22} + 2\delta w_{,12} M_{12} \\ &= \int_{\Omega} \nabla \delta w_{,1} \cdot \begin{pmatrix} M_{11} \\ M_{12} \end{pmatrix} + \nabla \delta w_{,2} \cdot \begin{pmatrix} M_{12} \\ M_{22} \end{pmatrix} = \int_{\partial\Omega} (\nabla \delta w)^T \begin{pmatrix} M_{11} & M_{12} \\ M_{12} & M_{22} \end{pmatrix} \mathbf{n} - C \end{aligned} \tag{A.1}$$

with

$$\begin{aligned} C &= \int_{\Omega} \delta w_{,1} \nabla \cdot \begin{pmatrix} M_{11} \\ M_{12} \end{pmatrix} + \delta w_{,2} \nabla \cdot \begin{pmatrix} M_{12} \\ M_{22} \end{pmatrix} = \int_{\Omega} \nabla \delta w \cdot \begin{pmatrix} M_{11,1} + M_{12,2} \\ M_{12,1} + M_{22,2} \end{pmatrix} \\ &= \int_{\partial\Omega} \delta w \begin{pmatrix} M_{11,1} + M_{12,2} \\ M_{12,1} + M_{22,2} \end{pmatrix} \cdot \mathbf{n} - \int_{\Omega} \delta w (M_{11,11} + M_{12,12} + M_{22,22}) \cdot \end{aligned} \tag{A.2}$$

Decomposing the boundary term in (A.1) using  $\nabla \delta w = (\nabla \delta w \cdot \mathbf{n}) \mathbf{n} + (\nabla \delta w \cdot \mathbf{s}) \mathbf{s}$  combined with (A.2) gives (4).

We now want to extract the boundary condition from the elastic term in the transformed version given by (20a). We can rewrite as the general form

$$\int_{\tilde{\Omega}} \tilde{D}(\delta W, W) = \int_{\tilde{\Omega}} \delta W_{,11} Q_{11} + \delta W_{,22} Q_{22} + \delta W_{,12} Q_{12} + \delta W_{,1} R_1 + \delta W_{,2} R_2.$$

The terms containing  $Q$  can be treated by an integration by parts as in (A.1) and we have

$$\int_{\tilde{\Omega}} \tilde{D}(\delta W, W) = \int_{\partial\tilde{\Omega}} (\nabla \delta W)^T \begin{pmatrix} Q_{11} & Q_{12} \\ Q_{12} & Q_{22} \end{pmatrix} \mathbf{n} - \tilde{C} \tag{A.3}$$

with

$$\tilde{C} = \int_{\tilde{\Omega}} \nabla \delta w \cdot \begin{pmatrix} Q_{11,1} + Q_{12,2} - R_1 \\ Q_{12,1} + Q_{22,2} - R_2 \end{pmatrix} = \int_{\partial\tilde{\Omega}} \delta w \begin{pmatrix} Q_{11,1} + Q_{12,2} - \tilde{R}_1 \\ Q_{12,1} + Q_{22,2} - \tilde{R}_2 \end{pmatrix} \cdot \mathbf{n} - \int_{\tilde{\Omega}} \delta w (Q_{11,11} + Q_{12,12} + Q_{22,22} - \tilde{R}_{1,1} - \tilde{R}_{2,2}). \tag{A.4}$$

Using the symmetry of  $D_{IJKL}$ , the last term in (A.4) gives the formulation in  $M_{IJ}$ ,  $N_{IJ}$  and  $S_I$  as in (22). The boundary term in (A.3) is decomposed with respect to the basis  $(\mathbf{n}, \mathbf{s})$ , so that

$$\int_{\partial\tilde{\Omega}} (\nabla \delta W)^T \begin{pmatrix} Q_{11} & Q_{12} \\ Q_{12} & Q_{22} \end{pmatrix} \mathbf{n} = \int_{\partial\tilde{\Omega}} \left( \mathbf{n}^T \begin{pmatrix} Q_{11} & Q_{12} \\ Q_{12} & Q_{22} \end{pmatrix} \mathbf{n} \right) (\nabla \delta W \cdot \mathbf{n}) + \left( \mathbf{s}^T \begin{pmatrix} Q_{11} & Q_{12} \\ Q_{12} & Q_{22} \end{pmatrix} \mathbf{n} \right) (\nabla \delta W \cdot \mathbf{s}). \tag{A.5}$$

Integrating by parts the term with  $\nabla W \cdot \mathbf{s}$  gives

$$\int_{\delta\tilde{\Omega}} \left( \mathbf{s}^T \begin{pmatrix} Q_{11} & Q_{12} \\ Q_{12} & Q_{22} \end{pmatrix} \mathbf{n} \right) (\nabla \delta W \cdot \mathbf{s}) = - \int_{\delta\tilde{\Omega}} \delta W \nabla \left( \mathbf{s}^T \begin{pmatrix} Q_{11} & Q_{12} \\ Q_{12} & Q_{22} \end{pmatrix} \mathbf{n} \right) \cdot \mathbf{s}. \tag{A.6}$$

Injecting (A.5) and (A.6) in (A.3) leads to (22).

### Appendix B. Computation on Jacobian of $F$

Consider the Jacobian of a change of coordinates  $F$  :

$$\mathbf{J} = \begin{pmatrix} F_{1,1} & F_{1,2} \\ F_{2,1} & F_{2,2} \end{pmatrix}.$$

Then we define  $\hat{\mathcal{J}} \in \mathbb{A}^{3 \times 3}$  such that for all  $\mathbf{U} \in \mathbb{A}^{3 \times 3}$  we have  $\widehat{\mathbf{J}^T \mathbf{U} \mathbf{J}} = \hat{\mathcal{J}} \mathbf{U}$  and

$$\hat{\mathcal{J}} = \begin{pmatrix} F_{1,1}^2 & F_{2,1}^2 & \sqrt{2}F_{1,1}F_{2,1} \\ F_{1,2}^2 & F_{2,2}^2 & \sqrt{2}F_{1,2}F_{2,2} \\ \sqrt{2}F_{1,1}F_{1,2} & \sqrt{2}F_{2,1}F_{2,2} & F_{1,1}F_{2,2} + F_{1,2}F_{2,1} \end{pmatrix}.$$

After computation of  $\hat{\mathcal{J}}^T \hat{\mathcal{J}}$  and noting  $\gamma = F_{1,1}F_{2,1} + F_{1,2}F_{2,2}$ , we have

$$\hat{\mathcal{J}}^T \hat{\mathcal{J}} = \begin{pmatrix} (F_{1,1}^2 + F_{1,2}^2)^2 & \gamma^2 & \sqrt{2}\gamma(F_{1,1}^2 + F_{1,2}^2) \\ \gamma^2 & (F_{2,1}^2 + F_{2,2}^2)^2 & \sqrt{2}\gamma(F_{2,1}^2 + F_{2,2}^2) \\ \sqrt{2}\gamma(F_{1,1}^2 + F_{1,2}^2) & \sqrt{2}\gamma(F_{2,1}^2 + F_{2,2}^2) & \gamma^2 + |\mathbf{J}|^2 \end{pmatrix}.$$

We also have

$$\widehat{\mathbf{J} \mathbf{J}^T \mathbf{J} \mathbf{J}^T} = \begin{pmatrix} 4F_{1,1}^2 F_{1,2}^2 & 4F_{1,1} F_{1,2} F_{1,2} F_{2,2} & 2\sqrt{2}F_{1,1} F_{1,2} \gamma \\ 4F_{1,1} F_{1,2} F_{1,2} F_{2,2} & 4F_{2,1}^2 F_{2,2}^2 & 2\sqrt{2}F_{2,1} F_{2,2} \gamma \\ 2\sqrt{2}F_{1,1} F_{1,2} \gamma & 2\sqrt{2}F_{2,1} F_{2,2} \gamma & 2\gamma^2 \end{pmatrix}.$$

### Appendix C. Cloaking a polynya

Following on from model (14), we can also look into using the space transformation method for cloaking a polynya (i.e. a hole of free water surface within the floating plate). Indeed, it has been pointed out by Greenleaf et al. [50] that some almost trapped eigenstates occur in the invisibility region created by a cloak in the context of matter waves. For water waves, the objective would be to find plate parameters in a cloak region around the polynya so as to reduce sloshing inside the polynya, which is a problem of interest in ocean engineering [51].

Compared to the case with a cylinder, in which there is no water in the domain occupied by the cylinder, application of the space transformation method for a polynya transforms the equations in the water domain underneath the polynya as well. In order to make the equations shape-invariant in the polynya region, we must consider a change in the seabed topography in this region as there are no plate parameters to adjust at the surface. Nevertheless, pursuing the idea of the transformation method, we suppose a change of coordinates that inflates a small polynya to a large one. It turns out that the transformation lowers the seabed underneath the small polynya, so it has to be a hill in order for it to be flat in the transformed region or, if it is flat in the untransformed region, it is an inverse hill in the transformed region.

More concretely, let us consider an anisotropic plate  $(\tilde{D}, \tilde{p})$  given by (38) with an inner hole of free surface. For example, by change of coordinates (37), we can identify this setup as a transformed version of a corresponding untransformed geometry consisting of a plate  $(D, p)$  given by (36) with a polynya of radius  $a_0 < a$  and a water depth  $d$  under the plate and  $a_0 d/a < d$  in the polynya region. As the scattering in the untransformed region is potentially large rather than small owing to the hill in the sea bed, this would create larger surface waves within the polynya and, unfortunately, the objective of energy minimisation in the polynya cannot be achieved.

Nevertheless, the case of starting with a flat seabed at the price of a trough in the sea bed underneath the polynya might be worth pursuing.

### Data availability

No data was used for the research described in the article.

## References

- [1] J.B. Pendry, D. Schurig, D.R. Smith, Controlling electromagnetic fields, *Science* 312 (5781) (2006) 1780–1782.
- [2] U. Leonhardt, Optical conformal mapping, *Science* 312 (5781) (2006) 1777–1780.
- [3] R. Fleury, A. Alu, Cloaking and invisibility: A review, in: *Forum for Electromagnetic Research Methods and Application Technologies*, Vol. 1, No. 1, FERMAT, 2014.
- [4] D. Schurig, J.J. Mock, B.J. Justice, S.A. Cummer, J.B. Pendry, A.F. Starr, D.R. Smith, Metamaterial electromagnetic cloak at microwave frequencies, *Science* 314 (5801) (2006) 977–980.
- [5] W. Cai, U.K. Chettiar, A.V. Kildishev, V.M. Shalaev, Optical cloaking with metamaterials, *Nat. Photonics* 1 (4) (2007) 224–227.
- [6] H. Chen, C.T. Chan, Acoustic cloaking in three dimensions using acoustic metamaterials, *Appl. Phys. Lett.* 91 (18) (2007).
- [7] S.A. Cummer, D. Schurig, One path to acoustic cloaking, *New J. Phys.* 9 (3) (2007) 45.
- [8] R. Porter, Cloaking in water waves, in: S. Maier, R. Craster, S. Guenneau (Eds.), *Handbook of Metamaterials and Plasmonics*, Vol. 2: Elastic, Acoustic, and Seismic Metamaterials, World Scientific Publishing Co. Singapore, 2017.
- [9] B. Davies, S. Sznyszewski, M.A. Dias, L. de Waal, A. Kisil, V.P. Smyshlyaev, S. Cooper, I.V. Kamotski, M. Touboul, R.V. Craster, et al., Roadmap on metamaterial theory, modelling and design, *J. Phys. D: Appl. Phys.* 58 (20) (2025) 203002.
- [10] R. Porter, Cloaking of a cylinder in waves, in: *Proceedings of 26th International Workshop on Water Waves and Floating Bodies*, Athens, Greece, 2011.
- [11] A. Zareei, M.-R. Alam, Cloaking in shallow-water waves via nonlinear medium transformation, *J. Fluid Mech.* 778 (2015) 273–287.
- [12] T. Iida, M. Kashiwagi, Water wave focusing using coordinate transformation, *J. Energy Power Eng.* 11 (2017) 631–636.
- [13] Z. Zhang, G. He, Y. Gou, Z. Luan, S. Liu, R. He, Wavelength manipulation in shallow water via space transformation method, *Phys. Fluids* 35 (11) (2023).
- [14] M. Farhat, S. Enoch, S. Guenneau, A. Movchan, Broadband cylindrical acoustic cloak for linear surface waves in a fluid, *Phys. Rev. Lett.* 101 (13) (2008) 134501.
- [15] H. Chen, J. Yang, J. Zi, C.T. Chan, Transformation media for linear liquid surface waves, *Europhys. Lett.* 85 (2) (2009) 24004.
- [16] P. Chamberlain, D. Porter, The modified mild-slope equation, *J. Fluid Mech.* 291 (1995) 393–407.
- [17] G. Dupont, S. Guenneau, O. Kimmoun, B. Molin, S. Enoch, Cloaking a vertical cylinder via homogenization in the mild-slope equation, *J. Fluid Mech.* 796 (2016) R1, <http://dx.doi.org/10.1017/jfm.2016.249>.
- [18] T. Iida, M. Kashiwagi, Small water channel network for designing wave fields in shallow water, *J. Fluid Mech.* 849 (2018) 90–110.
- [19] C. Berraquero, A. Maurel, P. Petitjeans, V. Pagneux, Experimental realization of a water-wave metamaterial shifter, *Phys. Rev. E—Statistical, Nonlinear, Soft Matter Phys.* 88 (5) (2013) 051002.
- [20] R. Porter, J. Newman, Cloaking of a vertical cylinder in waves using variable bathymetry, *J. Fluid Mech.* 750 (2014) 124–143.
- [21] J. Newman, Cloaking a circular cylinder in water waves, *Eur. J. Mech. B Fluids* 47 (2014) 145–150.
- [22] T. Iida, A. Zareei, M.-R. Alam, Water wave cloaking using a floating composite plate, *J. Fluid Mech.* 954 (2023) A4.
- [23] G.W. Milton, M. Briane, J.R. Willis, On cloaking for elasticity and physical equations with a transformation invariant form, *New J. Phys.* 8 (10) (2006) 248.
- [24] M. Farhat, S. Guenneau, S. Enoch, A.B. Movchan, Cloaking bending waves propagating in thin elastic plates, *Phys. Rev. B* 79 (3) (2009) 033102.
- [25] D.J. Colquitt, M. Brun, M. Gei, A.B. Movchan, N.V. Movchan, I.S. Jones, Transformation elastodynamics and cloaking for flexural waves, *J. Mech. Phys. Solids* 72 (2014) 131–143.
- [26] N. Stenger, M. Wilhelm, M. Wegener, Experiments on elastic cloaking in thin plates, *Phys. Rev. Lett.* 108 (1) (2012) 014301.
- [27] D. Misseroni, D.J. Colquitt, A.B. Movchan, N.V. Movchan, I.S. Jones, Cymatics for the cloaking of flexural vibrations in a structured plate, *Sci. Rep.* 6 (1) (2016) 23929.
- [28] K. Tang, E. Luz, D. Amram, L. Kadysz, S. Guenneau, P. Sebbah, Dynamic cloaking of a diamond-shaped hole in elastic plate, *Appl. Phys. Lett.* 122 (1) (2023).
- [29] M. Brun, D. Colquitt, I. Jones, A. Movchan, N. Movchan, Transformation cloaking and radial approximations for flexural waves in elastic plates, *New J. Phys.* 16 (9) (2014) 093020.
- [30] A. Zareei, M.-R. Alam, Broadband cloaking of flexural waves, *Phys. Rev. E* 95 (6) (2017) 063002.
- [31] L. Pomot, S. Bourgeois, C. Payan, M. Remillieux, S. Guenneau, On form invariance of the Kirchhoff-Love plate equation, 2019, arXiv preprint arXiv:1901.00067.
- [32] D. Porter, R. Porter, Approximations to wave scattering by an ice sheet of variable thickness over undulating bed topography, *J. Fluid Mech.* 509 (2004) 145–179.
- [33] L. Bennetts, N. Biggs, D. Porter, A multi-mode approximation to wave scattering by ice sheets of varying thickness, *J. Fluid Mech.* 579 (2007) 413–443.
- [34] K. Sab, A. Lebé, Homogenization of heterogeneous thin and thick plates, John Wiley & Sons, 2015.
- [35] Y. Zhou, K. Huang, On simplified deformation gradient theory of modified gradient elastic Kirchhoff-Love plate, *Eur. J. Mech. A Solids* 100 (2023) 105014.
- [36] V.I. Gorbachev, L. Kabanova, Formulation of problems in the general Kirchhoff-Love theory of inhomogeneous anisotropic plates, *Mosc. Univ. Mech. Bull.* 73 (2018) 60–66.
- [37] G. Zilman, T. Miloh, Hydroelastic buoyant circular plate in shallow water: a closed form solution, *Appl. Ocean Res.* 22 (2000) 191–198.
- [38] G.B. Whitham, Variational methods and applications to water waves, *Proc. R. Soc. Lond. Ser. A. Math. Phys. Sci.* 299 (1456) (1967) 6–25.
- [39] J.W. Miles, On Hamilton's principle for surface waves, *J. Fluid Mech.* 83 (1) (1977) 153–158.
- [40] R. Porter, An extended linear shallow-water equation, *J. Fluid Mech.* 876 (2019) 413–427.
- [41] D. Lannes, On the dynamics of floating structures, *Ann. PDE* 3 (1) (2017) 11.
- [42] M. Kadic, G.W. Milton, M. van Hecke, M. Wegener, 3D metamaterials, *Nat. Rev. Phys.* 1 (3) (2019) 198–210.
- [43] R. Craster, S. Guenneau, M. Kadic, M. Wegener, Mechanical metamaterials, *Rep. Progr. Phys.* 86 (9) (2023) 094501.
- [44] L. Bourgeois, L. Chesnel, S. Fliss, On well-posedness of time-harmonic problems in an unbounded strip for a thin plate model, 2018, arXiv preprint arXiv:1809.10950.
- [45] L. Bourgeois, C. Hazard, On well-posedness of scattering problems in a Kirchhoff-Love infinite plate, *SIAM J. Appl. Math.* 80 (3) (2020) 1546–1566, <http://dx.doi.org/10.1137/19M1295660>.
- [46] L. Pomot, C. Payan, M. Remillieux, S. Guenneau, Acoustic cloaking: Geometric transform, homogenization and a genetic algorithm, *Wave Motion* 92 (2020) 102413.
- [47] M. Brun, S. Guenneau, A.B. Movchan, Achieving control of in-plane elastic waves, *Appl. Phys. Lett.* 94 (6) (2009).
- [48] R.V. Kohn, H. Shen, M.S. Vogelius, M.I. Weinstein, Cloaking via change of variables in electric impedance tomography, *Inverse Problems* 24 (1) (2008) 015016.
- [49] M.A. Peter, M.H. Meylan, H. Chung, Wave scattering by a circular elastic plate in water of finite depth: a closed form solution, *Int. J. Offshore Polar Eng.* 14 (2004) 81–85.
- [50] A. Greenleaf, Y. Kurylev, M. Lassas, G. Uhlmann, Approximate quantum cloaking and almost-trapped states, *Phys. Rev. Lett.* 101 (22) (2008) 220404.
- [51] B. Molin, On the piston and sloshing modes in moonpools, *J. Fluid Mech.* 430 (2001) 27–50.